TEOBREsumS: an Effective-One-Body waveform model for coalescing black hole binaries

Angelica Albertini

Astronomical Institute of the Czech Academy of Sciences

Prague Relativity Group meeting

3rd of December, 2021

Outline

- The **Effective-One-Body** approach to the two-body problem in GR
- **TEOBResumS**: Effective-One-Body waveform model for nonprecessing coalescing black hole binaries on quasi-circular orbits

Waveforms and fluxes: Towards a self-consistent effective one body waveform model for nonprecessing, coalescing black-hole binaries for third generation detectors

Angelica Albertini[1,2], Alessandro Nagar[3,4], Piero Rettegno[3,5], Simone Albanesi[3,5], and Rossella Gamba[6]

[1] *Astronomical Institute of the Czech Academy of Sciences, Boční II 1401/1a, CZ-141 00 Prague, Czech Republic*

[2] *Faculty of Mathematics and Physics, Charles University in Prague, 18000 Prague, Czech Republic*

[3] *INFN Sezione di Torino, Via P. Giuria 1, 10125 Torino, Italy*

[4] *Institut des Hautes Etudes Scientifiques, 91440 Bures-sur-Yvette, France*

[5] *Dipartimento di Fisica, Università di Torino, via P. Giuria 1, 10125 Torino, Italy and*

[6] *Theoretisch-Physikalisches Institut, Friedrich-Schiller-Universität Jena, 07743, Jena, Germany*

We present a comprehensive comparison between numerical relativity (NR) angular momentum fluxes at infinity and the corresponding quantity entering the radiation reaction in `TEOBResumS`, an Effective-One-Body (EOB) waveform model for nonprecessing coalescing black hole binaries on quasi-circular orbits. This comparison prompted us to implement two changes in the model: (i) including Next-to-Quasi-Circular corrections in the $\ell = m$, $\ell \leq 5$ multipoles entering the radiation reaction and (ii) consequently updating the NR-informed spin-orbital sector of the model. This yields a new waveform model that presents a higher self-consistency between waveform and dynamics and an improved agreement with NR simulations. We test the model computing the EOB/NR unfaithfulness $\bar{F}_{\rm EOB/NR}$ over all 534 spin-aligned configurations available through the Simulating eXtreme Spacetime catalog, notably using the noise spectral density of Advanced LIGO, Einstein Telescope and Cosmic Explorer, for total mass up to $500M_\odot$. We find that the maximum unfaithfulness $\bar{F}^{\rm max}_{\rm EOB/NR}$ is mostly between 10^{-4} and 10^{-3}, and the performance progressively worsens up to $\sim 5 \times 10^{-3}$ as the effective spin of the system is increased. We perform similar analyses on the `SEOBNRv4HM` model, that delivers $\bar{F}^{\rm max}_{\rm EOB/NR}$ values uniformly distributed versus effective spin and mostly between 10^{-3} and 10^{-2}. We conclude that the improved `TEOBResumS` model already represents a reliable and robust first step towards the development of highly accurate waveform templates for third generation detectors.

arXiv:2111.14149 [gr-qc]

Compact binary coalescences

- Coalescence of two compact objects (BH/NS):
  emission of **gravitational radiation**
- Faithful waveform templates needed to **detect the signal** through matched filtering and infer the sources parameters
- Einstein's equations can be solved numerically
  -> but high computational costs
  -> impossible to cover the whole parameter space
- Analytical approaches: allow a **fast and accurate waveform generation**

The two-body problem in General Relativity

Classical approaches

Post **N**ewtonian expansion	**P**ost **M**inkowskian expansion	Black Hole perturbation theory
$(v/c)^2$	G	
slow velocity regime	weak field, any velocity	test-mass
any mass ratio	any mass ratio	any velocity
valid in the near zone	valid in the far zone	

The Effective-One-Body formalism

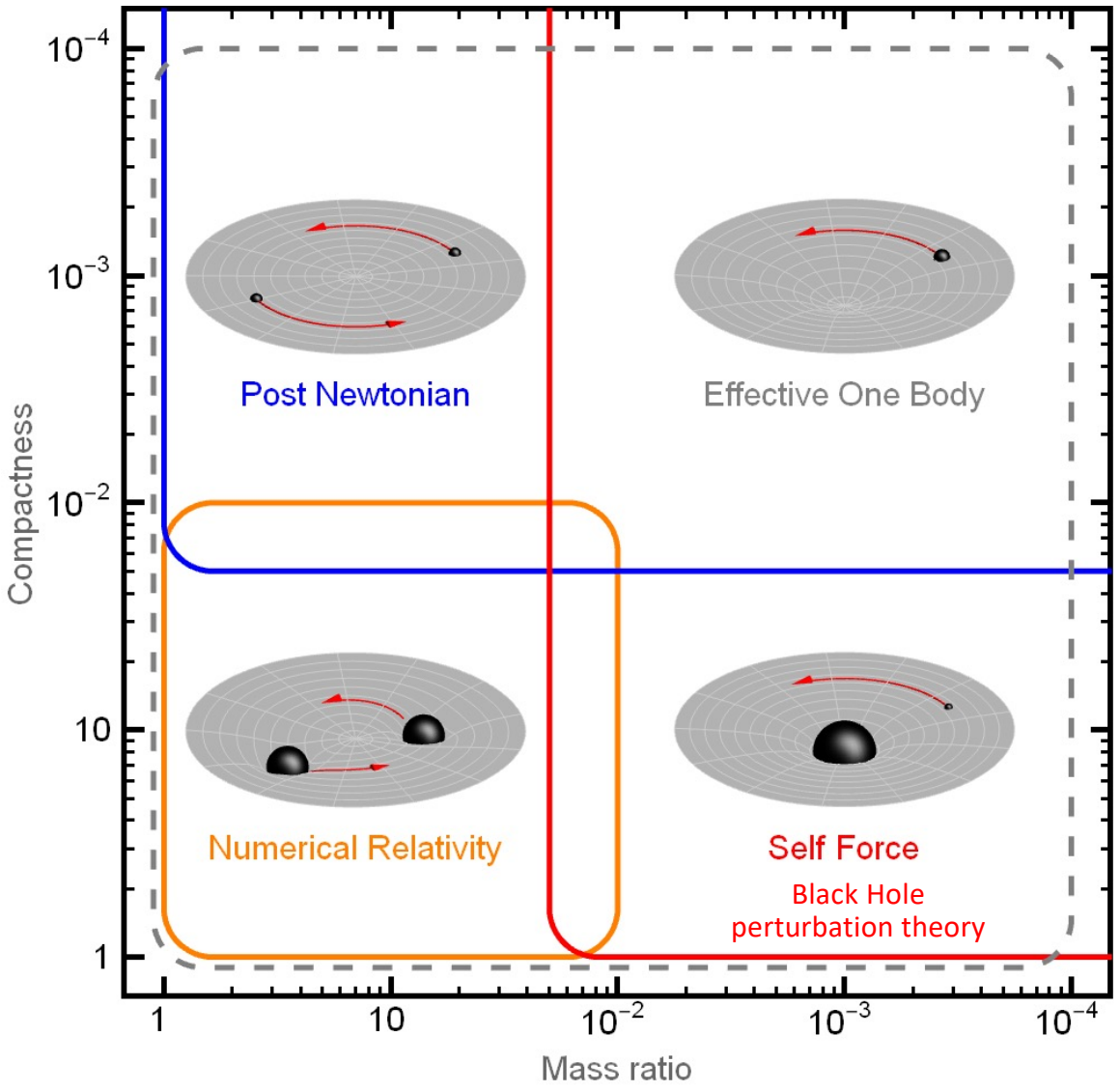

Theoretical results from classical approaches

Information from **N**umerical **R**elativity

EOB

flexible analytical approach, mapping the two-body dynamics in the motion of a particle with the reduced mass of the system moving in an effective metric (deformation of Schwarzschild/Kerr)

Theoretical framework

Mass ratio $q = \frac{m_1}{m_2}, \quad m_1 > m_2$

Symmetric mass ratio $\nu \equiv \frac{\mu}{M} = \frac{m_1 m_2}{(m_1 + m_2)^2}$

- Hamiltonian: conservative dynamics

  → found by mapping the "energy levels" of the real problem at a given PN order to the effective ones: $\mathscr{E}_{\rm eff} = \frac{\mathscr{E}^2 - m_1^2 c^4 - m_2^2 c^4}{2Mc^2}$

- Radiation reaction force $\hat{\mathscr{F}}_\varphi$: allows the orbit to shrink and circularize

- Full waveform: inspiral + merger + ringdown

  plunge (smooth transition)

Dynamical background

$G = c = 1$

Tortoise rescaled variables:

$$r_* = \int dr (A/B)^{1/2} \quad p_{r_*} = (A/B)^{1/2} p_r$$

Dimensionless EOB phase space variables on the equatorial plane:

$$r = \frac{R}{M}, \quad p_{r_*} = \frac{P_{R_*}}{\mu}, \quad p_\varphi = \frac{P_\varphi}{\mu M}, \quad t = \frac{T}{M}$$

$$\hat{H}_{\rm EOB} \equiv \frac{H_{\rm EOB}}{\mu} = \frac{1}{\nu}\sqrt{1 + 2\nu\left(\hat{H}_{\rm eff} - 1\right)} \qquad \hat{H}_{\rm eff} = \sqrt{p_{r_*}^2 + A(r,\nu)\left(1 + \frac{p_\varphi^2}{r^2} + 2\nu(4-3\nu)p_{r_*}^4\right)}$$

Continuous deformation in ν of a Schwarzschild metric:

$$ds^2_{\rm eff} = g^{\rm eff}_{\mu\nu} dx^\mu_{\rm eff} dx^\nu_{\rm eff} = -A(r)dt^2 + B(r)dR^2 + R^2(d\theta^2 + \sin^2\theta d\varphi^2)$$

$u = 1/r$

$$A^{\rm PN}_{\rm orb}(u) = 1 - 2u + 2\nu u^3 + \nu a_4 u^4 + \nu\left[a_5^c(\nu) + a_5^{\log}\ln u\right]u^5 + \nu\left[a_6^c(\nu) + a_6^{\log}\ln u\right]u^6$$

A potential

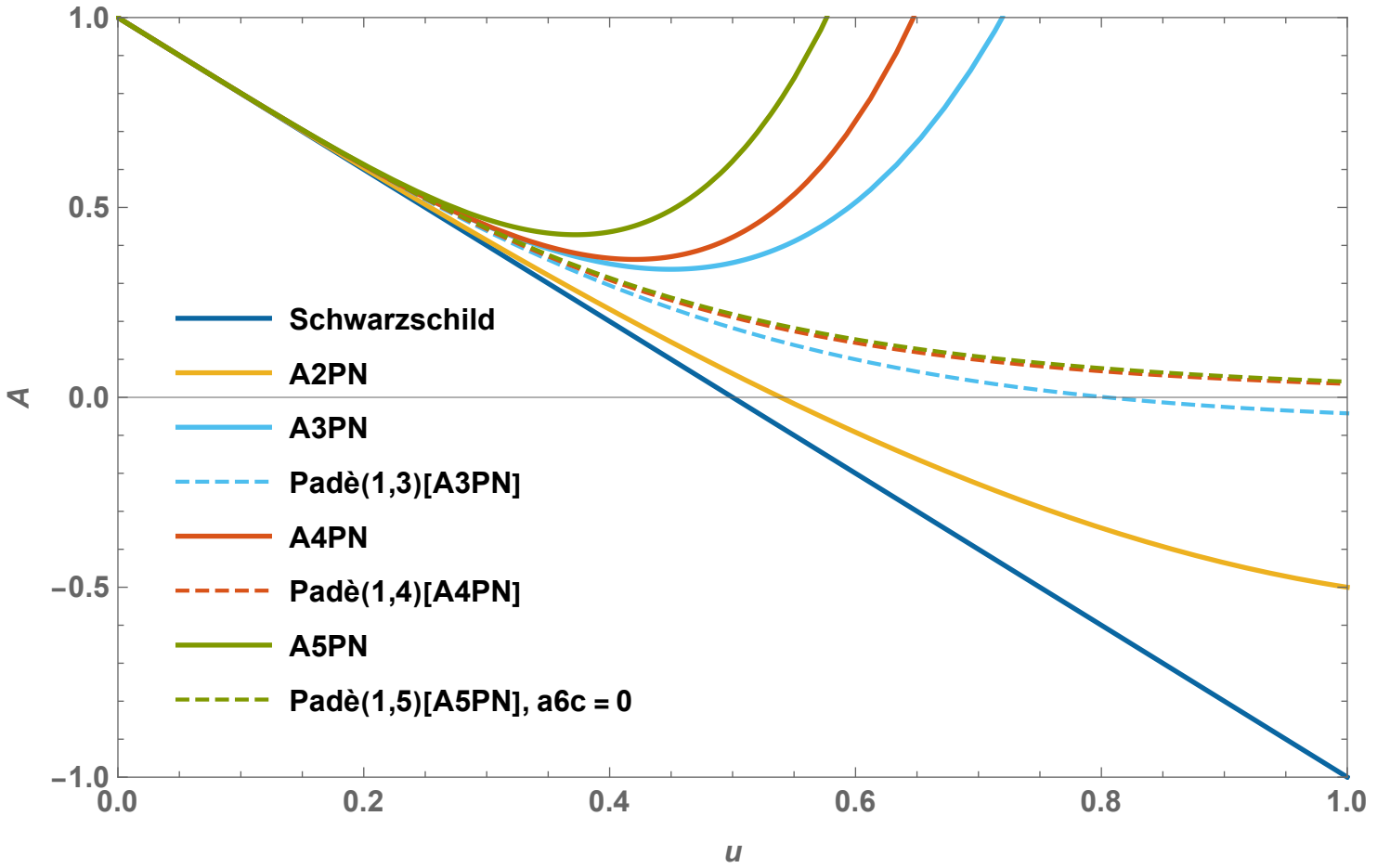

PN expansions: from 3PN on, the function no longer has a zero corresponding to the BH horizon in the test-particle limit

Padè resummation: ensures the function has the same qualitative behaviour as the test-particle limit

$$P_d^n[f(x)] = \frac{1 + a_1 x + \ldots + a_n x^n}{1 + b_1 x + \ldots + b_d x^d}$$

TEOBResumS: $A(u;\nu;a_6^c) = P_5^1\left[A_{\rm orb}^{\rm PN}(u)\right]$

NR-informing the EOB pt. I

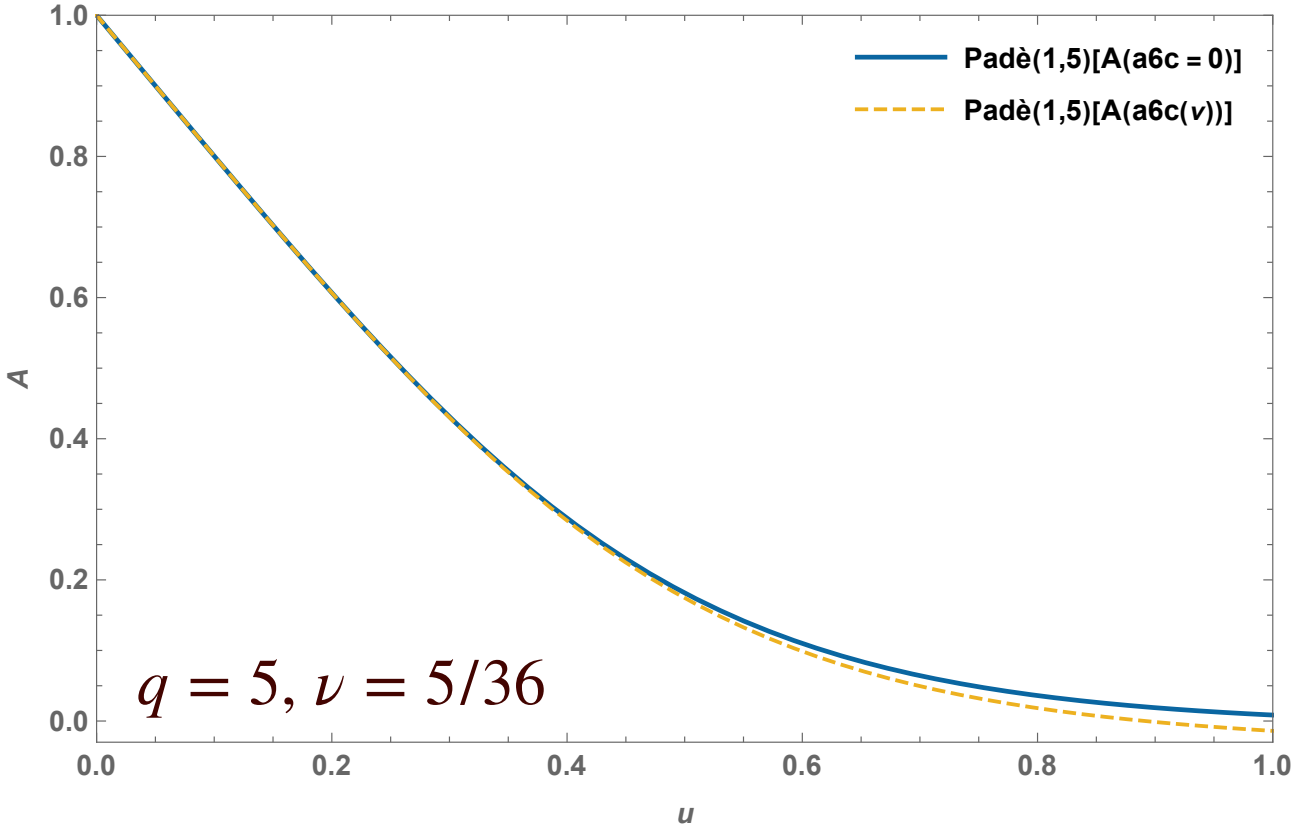

$$a_6^c(\nu) = n_0 \frac{1 + n_1\nu + n_2\nu^2 + n_3\nu^3}{1 + d_1\nu}$$

effective parameter tuned to numerical simulations

$$(q, \chi_1, \chi_2) = (2,0,0)$$

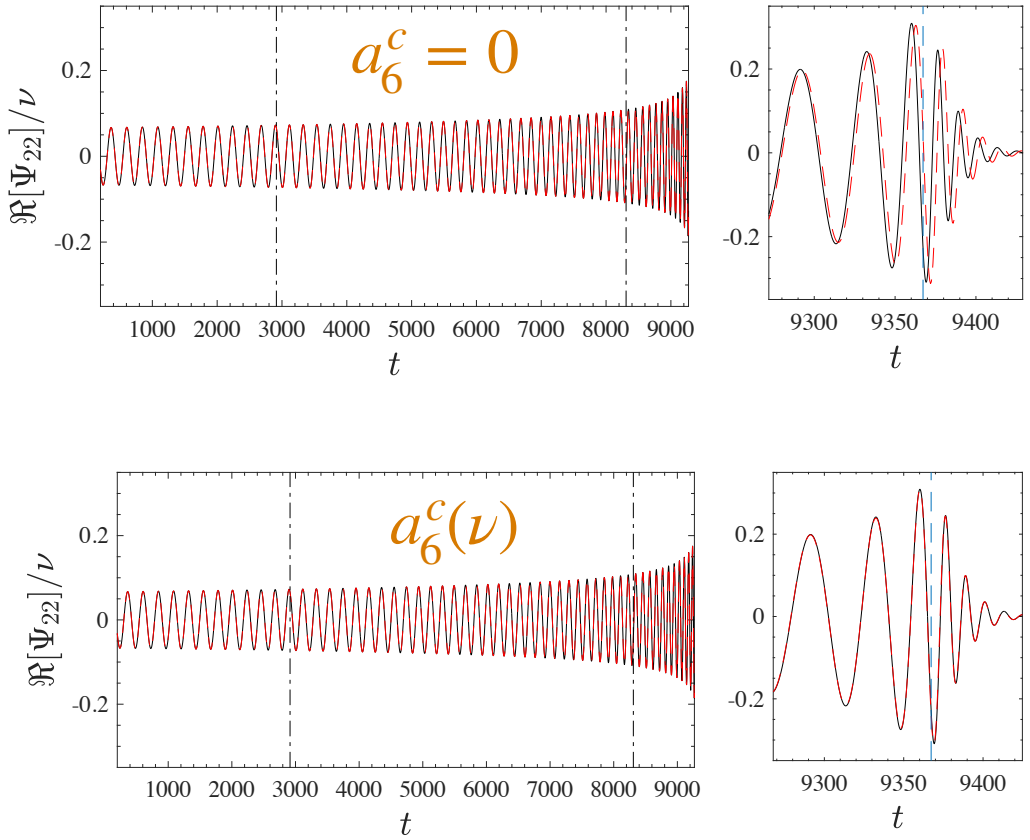

Spinning Black Holes

Dimensionless spins $\chi_i = \dfrac{S_i}{M_i^2}, \quad i = 1,2$

Deformation of a Kerr background:

$S = S_1 + S_2$ $\quad \hat{S} \equiv \dfrac{S}{M^2}$ spin of the primary

$S_* = \dfrac{M_2}{M_1} S_1 + \dfrac{M_1}{M_2} S_2$ $\quad \hat{S}_* \equiv \dfrac{S_*}{M^2}$ spin of the secondary

$X_1 = \dfrac{m_1}{M} = \dfrac{1}{2}\left(1 + \sqrt{1 - 4\nu}\right)$ $\quad X_2 = \dfrac{m_2}{M} = 1 - X_1$ $\quad X_{12} = X_1 - X_2$ $\quad \tilde{a}_i \equiv \chi_i X_i$

Dimensionless effective Kerr parameter: $\tilde{a}_0 = \tilde{a}_1 + \tilde{a}_2 = \chi_1 X_1 + \chi_2 X_2$

Centrifugal radius: $r_c^2 = r^2 + \tilde{a}_0^2\left(1 + \dfrac{2}{r}\right) + \delta\hat{a}^2$ spin-spin contribution

$\hat{H}_{\rm eff} = \hat{H}_{\rm eff}^{\rm orb} + p_\varphi\left(G_S \hat{S} + G_{S_*} \hat{S}_*\right)$

gyro-gravitomagnetic functions
(spin-orbit interaction)

$\hat{H}_{\rm eff}^{\rm orb} = \sqrt{p_{r_*}^2 + A\left(1 + \dfrac{p_\varphi^2}{r_c^2} + 2\nu(4 - 3\nu)\dfrac{p_{r_*}^4}{r_c^2}\right)}$

NR-informing the EOB pt. II

$$c_3(\tilde{a}_1,\tilde{a}_2,\nu) = p_0 \frac{1 + n_1\tilde{a}_0 + n_2\tilde{a}_0^2 + n_3\tilde{a}_0^3 + n_4\tilde{a}_0^4}{1 + d_1\tilde{a}_0} + p_1\tilde{a}_0\nu\sqrt{1-4\nu} + p_2\left(\tilde{a}_1 - \tilde{a}_2\right)\nu^2$$

effective parameter tuned to numerical simulations

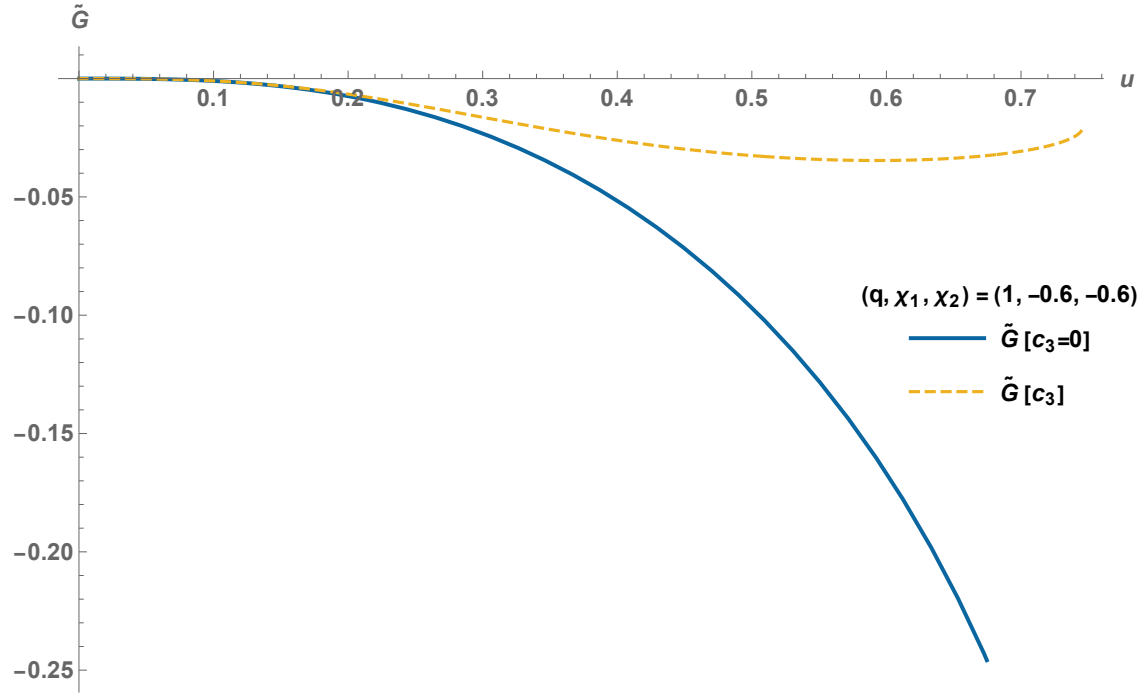

$$G_S = G_S^0 \hat{G}_S, \qquad G_S^0 = 2uu_c^2 \qquad \hat{G}_S = \frac{1}{1 + c_{10}u_c + c_{20}u_c^2 + c_{30}u_c^3 + c_{02}p_{r*}^2 + c_{12}u_c p_{r*}^2 + c_{04}p_{r*}^4}$$

$c_{30} = \nu c_3$

$$G_{S_*} = G_{S_*}^0 \hat{G}_{S_*}, \quad G_{S_*}^0 = (3/2)u_c^2 \qquad \hat{G}_{S_*} = \frac{1}{1 + c_{10}^* u_c + c_{20}^* u_c^2 + c_{30}^* u_c^3 + c_{40}^* u_c^4 + c_{02}^* p_{r*}^2 + c_{12}^* u_c p_{r*}^2 + c_{04}^* p_{r*}^4}$$

$c_{30}^* = \frac{135}{32} + \nu c_3$

Hamiltonian equations of motion

$$\frac{d\varphi}{dt} = \frac{\partial \hat{H}_{\mathrm{EOB}}}{\partial p_\varphi} = \Omega$$

Orbital frequency

$$\frac{dr}{dt} = \left(\frac{A}{B}\right)^{1/2} \frac{\partial \hat{H}_{\mathrm{EOB}}}{\partial p_{r_*}}$$

$$\frac{dp_\varphi}{dt} = \hat{\mathcal{F}}_\varphi$$

Radiation reaction

$$\frac{dp_{r_*}}{dt} = -\left(\frac{A}{B}\right)^{1/2} \frac{\partial \hat{H}_{\mathrm{EOB}}}{\partial r}$$

System of ODEs
-> solved numerically with ODE solver

Initial conditions: found via the Post-Adiabatic approximation
-> lowers initial eccentricity
-> allows to increase computational speed

Radiation Reaction

$$\dot{J}_{\rm system} = \hat{\mathscr{F}}_\varphi = -\dot{J}_\infty - \dot{J}_{\rm H_1} - \dot{J}_{\rm H_2} \qquad \hat{\mathscr{F}}_\varphi = \hat{\mathscr{F}}^\infty_\varphi + \hat{\mathscr{F}}^{\rm H}_\varphi$$

horizon contribution

asymptotic contribution

$$\hat{\mathscr{F}}^\infty_\varphi = -\frac{32}{5}\nu\, r_\omega^4\, \Omega^5\, \hat{f}^\infty\,(v_\varphi^2;\nu) \qquad 1 = \Omega^2 r_\omega^3$$

Modified Kepler's law valid during the plunge

Reduced flux function: $\hat{f}^\infty = \dfrac{1}{\mathscr{F}^{\rm Newt}_{22}} \sum_{\ell m} \mathscr{F}_{\ell m}$

energy flux radiated at infinity

$$\mathscr{F}_{\ell m} = \mathscr{F}^{\rm Newt}_{\ell m} \left|\hat{h}_{\ell m}\right|^2 \mathscr{F}^{\rm NQC}_{\ell m}$$

correction from the waveform

Inspiral + plunge waveform

$$h_+ - i h_\times = \frac{1}{\mathscr{D}_L} \sum_{\ell=2}^{\infty} \sum_{m=-\ell}^{\ell} h_{\ell m} \, {}_{-2}Y_{\ell m}(\theta, \varphi)$$

spherical harmonic modes (aka "multipoles")

$$x = v_\varphi^2 \equiv (r_\omega \Omega)^2$$

$$\ell_{\max} = 8$$

Newtonian prefactor

Resummed PN correction

Next-to-Quasi-Circular corrections

$$h_{\ell m} = h_{\ell m}^{(N,\epsilon)} \hat{S}_{\text{eff}}^{\epsilon} \, \hat{h}_{\ell m}^{\text{tail}}(x) \, \left[\rho_{\ell m}(x)\right]^{\ell} \, \hat{h}_{\ell m}^{\text{NQC}}$$

computed with the phase space variables found by solving the Hamiltonian equations of motion

Included up to $\ell = m = 5$ in the waveform and in the $\ell = m = 2$ mode of the radiation reaction

$$\mathscr{F}_{\ell m}^{\text{NQC}} = \left| \hat{h}_{\ell m}^{\text{NQC}} \right|^2$$

gravitational wave frequency

$$\omega_{\ell m} = \dot{\phi}_{\ell m}$$

Regge-**W**heeler-**Z**erilli normalized waveform

$$\Psi_{\ell m} \equiv \frac{h_{\ell m}}{\sqrt{(l+2)(l+1)l(l-1)}} = A_{\ell m} e^{-i\phi_{\ell m}}$$

Complete waveform

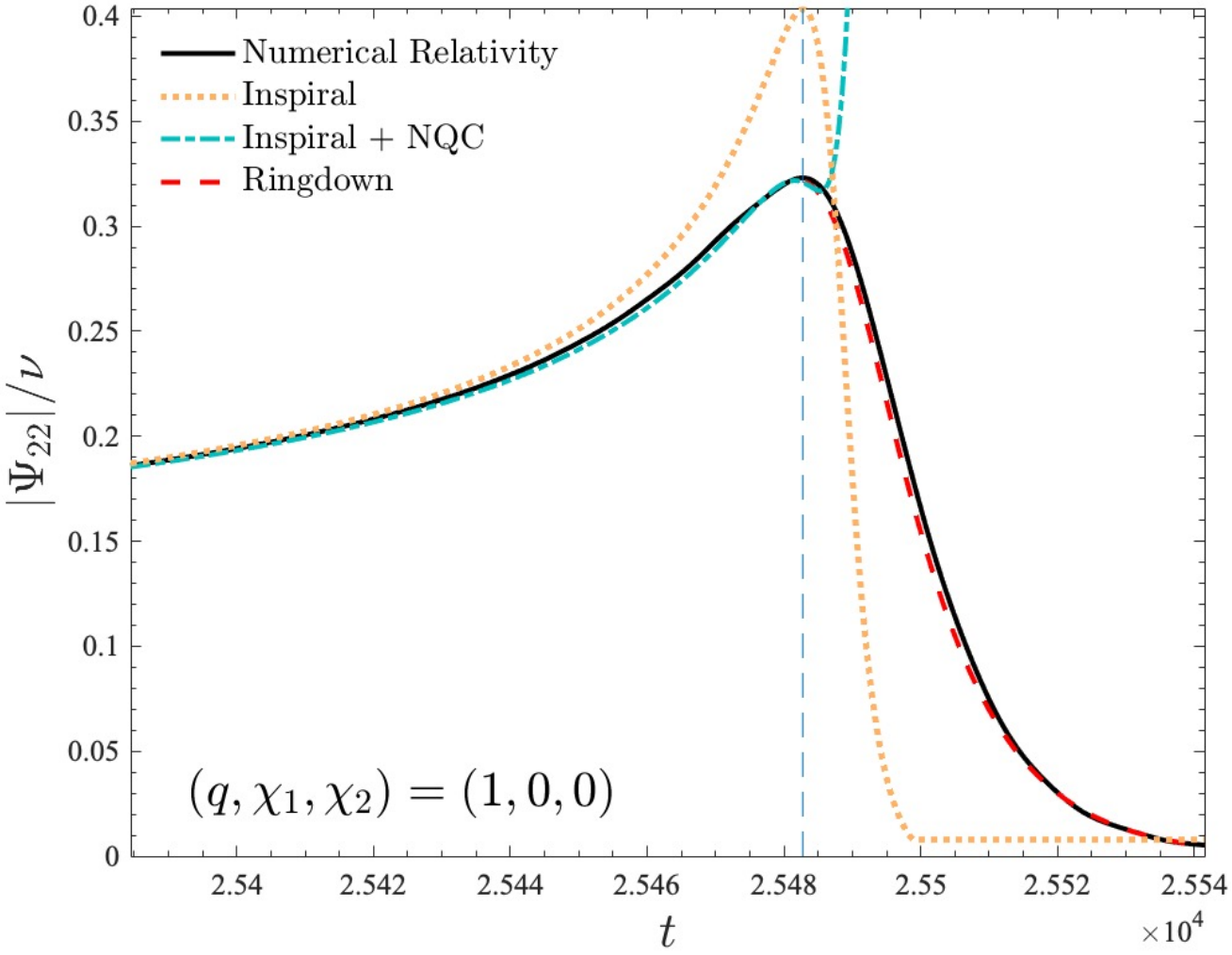

Inspiral+plunge waveform attached to the ringdown

theoretical results from BH perturbation theory + fit on the post merger phase of numerical simulations

Improving the EOB model TEOBResumS

- Checking the **dynamical self-consistency** of the model:
  agreement between orbital frequency and waveform frequency
- Comparison of **angular momentum flux** + development of a “cleaning” method to remove spurious oscillations from numerical curves
- To improve the agreement with numerical relativity:
  - addition of **Next-to-Quasi-Circular corrections** in the radiation reaction
  - new calibration of the **effective spin-orbit parameter c_3**
- Result: increased faithfulness of the dynamics and of the waveform

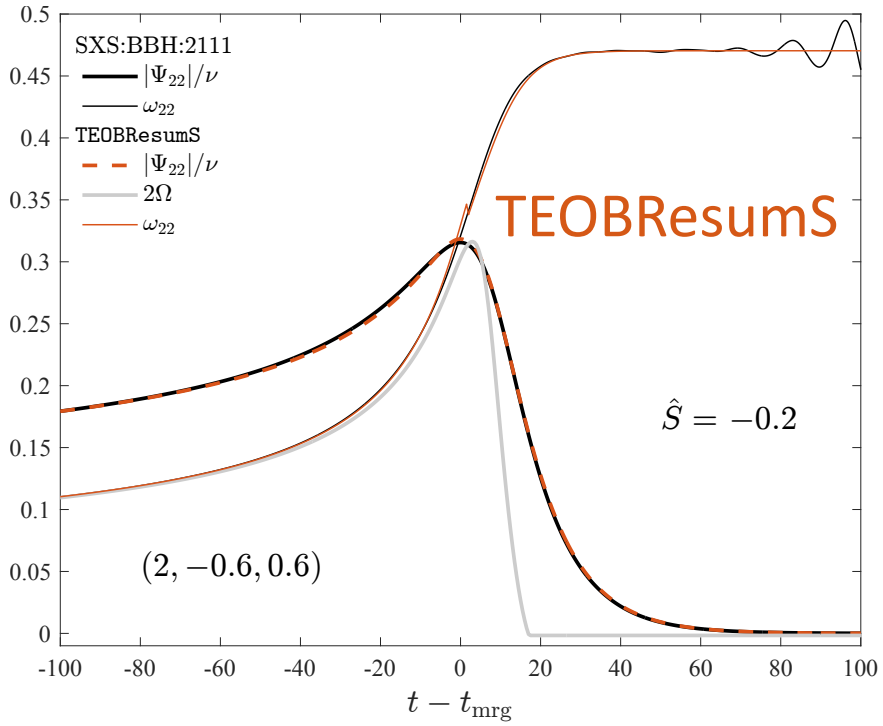

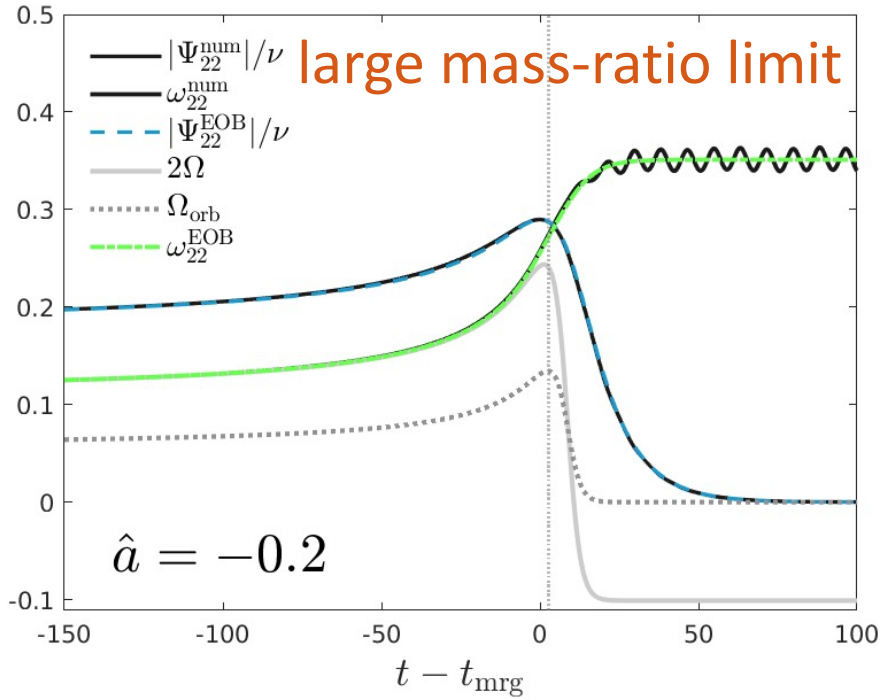

Orbital frequency

- 2Ω correctly grows as ω_{22}
  -> dynamical self-consistency
- qualitative agreement with the large-mass-ratio limit ($\nu = 10^{-3}$) for $\hat{a} = \hat{S}$
- TEOBResumS is built consistently with test-mass results -> good starting point to build a model for extreme-mass-ratios

$$S = S_1 + S_2 \qquad \hat{S} \equiv \frac{S}{M^2}$$

Angular momentum flux: Numerical Relativity

Angular momentum flux radiated at infinity: $\dot{J}^{\infty}_{\rm tot} = -\frac{1}{8\pi}\sum_{\ell,m} m\Im\left(\dot{h}_{\ell m}h^{*}_{\ell m}\right)$

EOB&NR both normalized to the Newtonian LO term: $\dot{J}^{\rm Newt}_{22} = \frac{32}{5}\nu^2\Omega^{7/3}$ $\qquad \Omega_{\rm NR} = \frac{\omega^{\rm NR}_{22}}{2}$

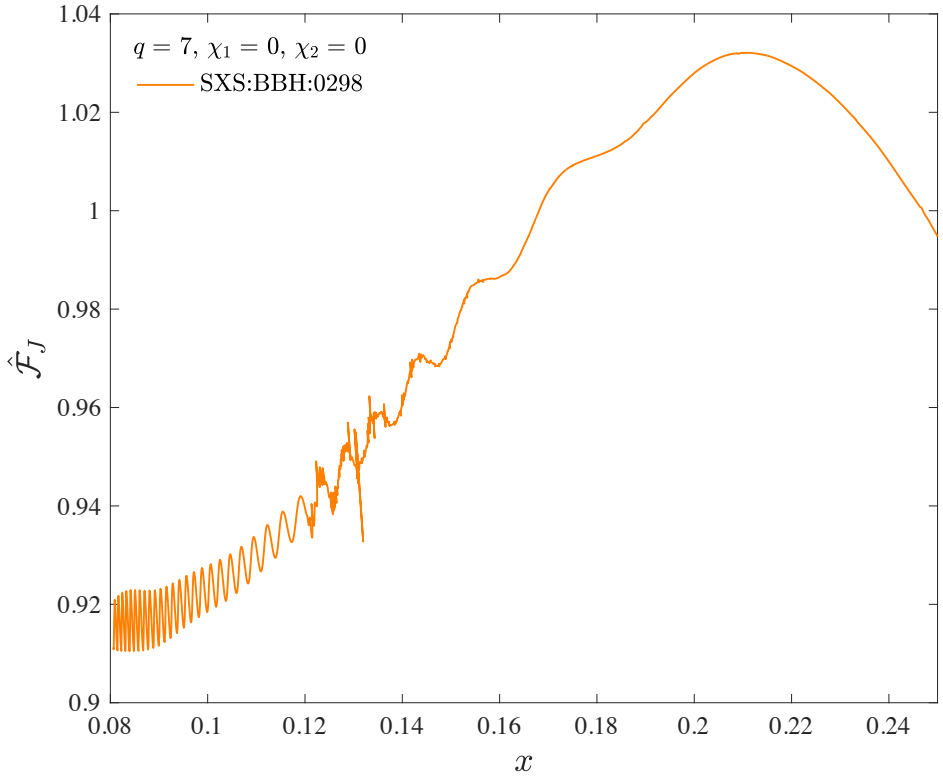

$x = \Omega^{2/3}$ frequency parameter

Numerical simulations publicly available from the **S**imulating e**X**treme **S**pacetimes catalog

Spurious oscillations in the initial part:

- Unclear comparison with other curves
- Impossibility to compute the relative difference / numerical accuracy

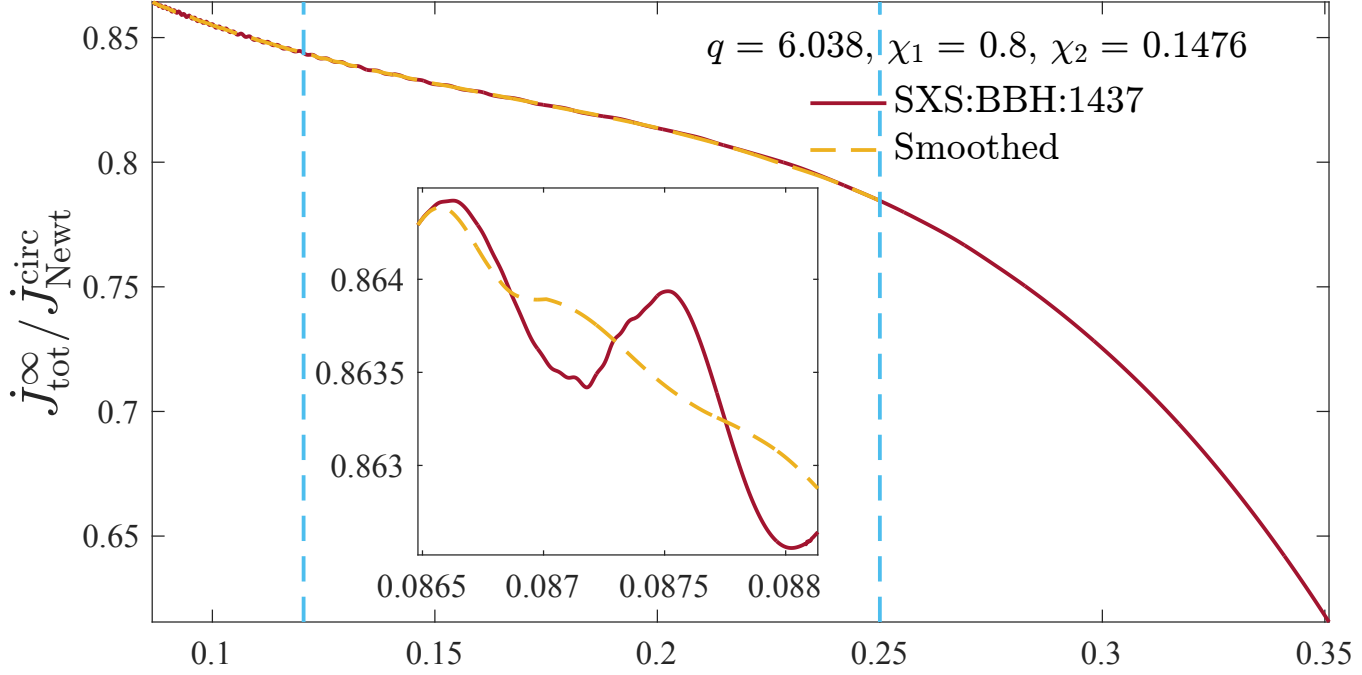

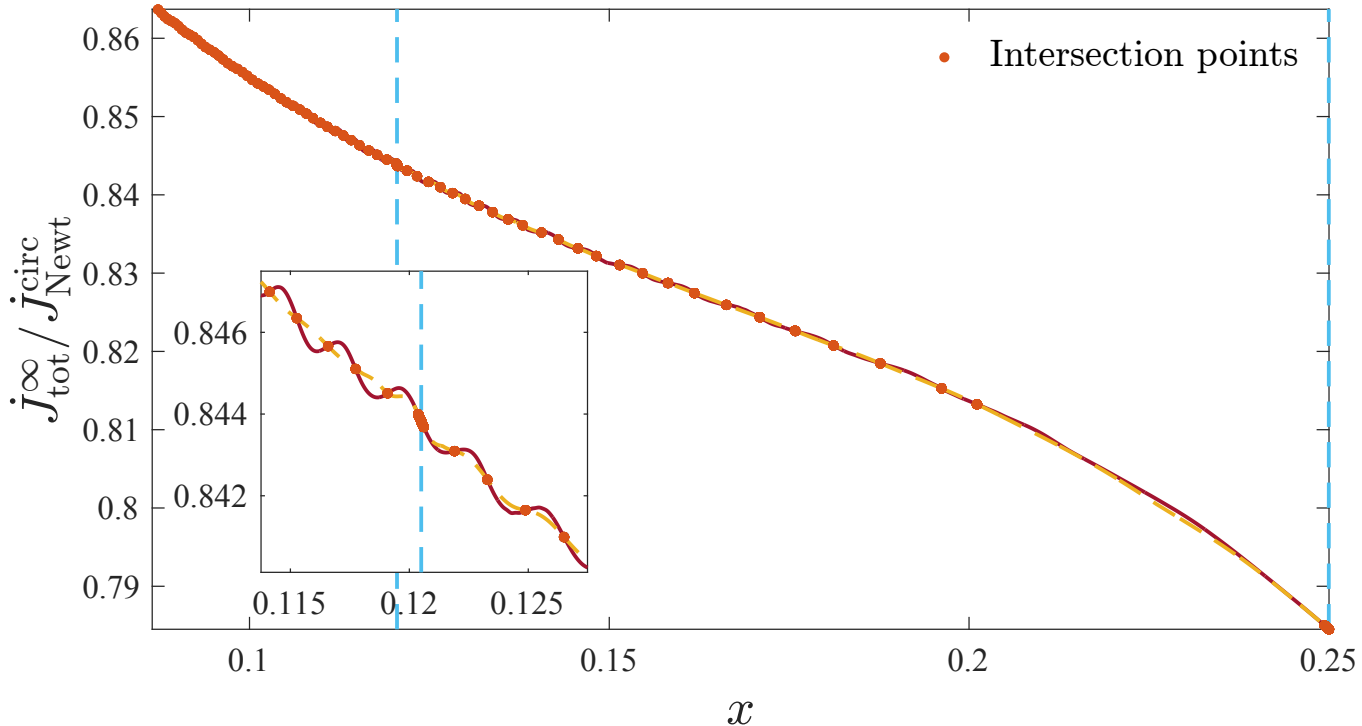

Cleaning

Key idea:

- smoothing the function
- finding the intersections between the original curve and the smoothed one
- fitting the points with a polynomial

Remarks:

- smoothing with a lowpass filter: different part of the curve have different spans
- last part of the curve left as it is

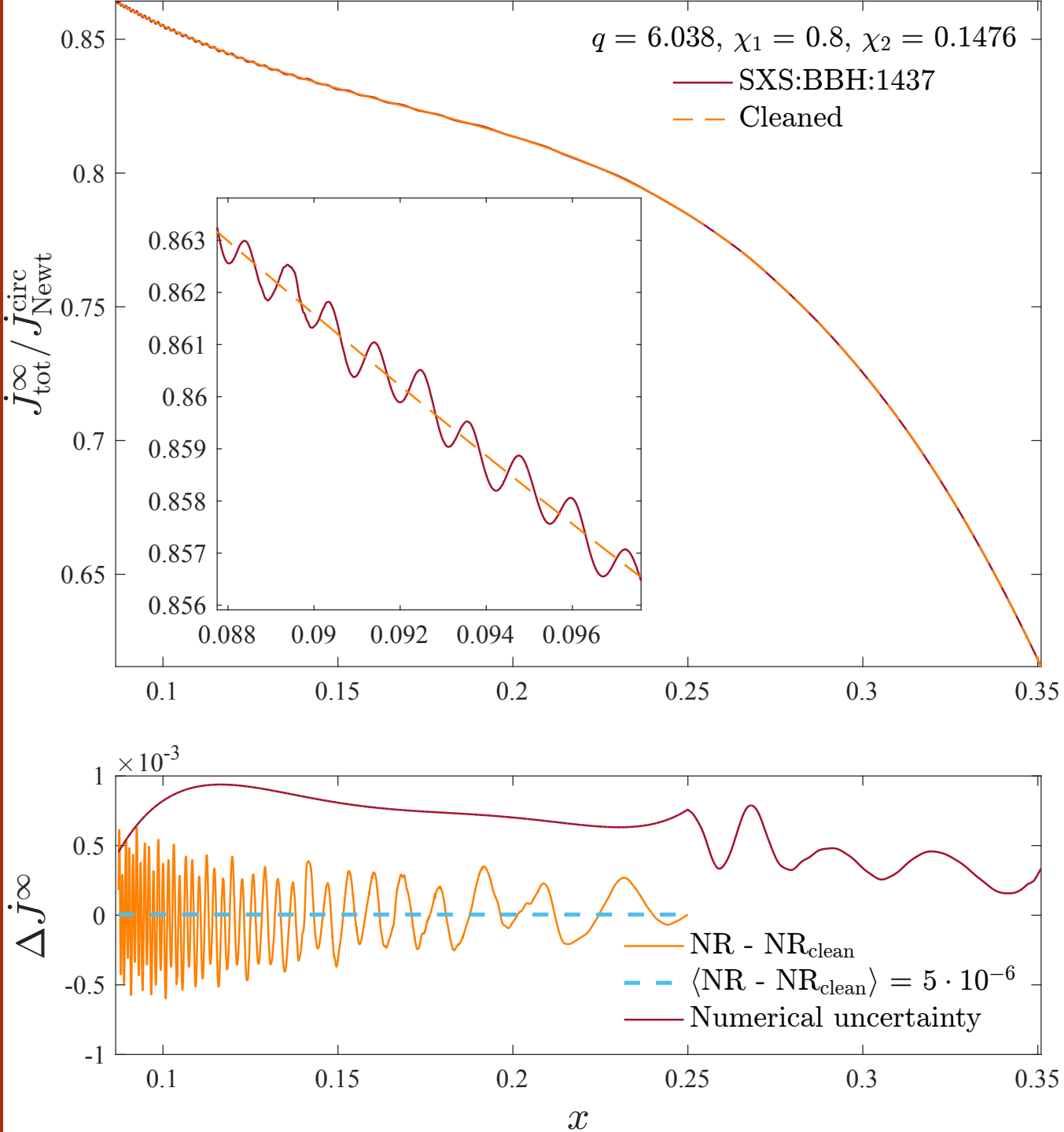

- Evaluating the difference with the original function: if it averages to zero, cleaning works out properly
- Numerical accuracy estimated with cleaned fluxes of the two higher available levels of resolution
- Cleaned flux can now be compared to EOB results

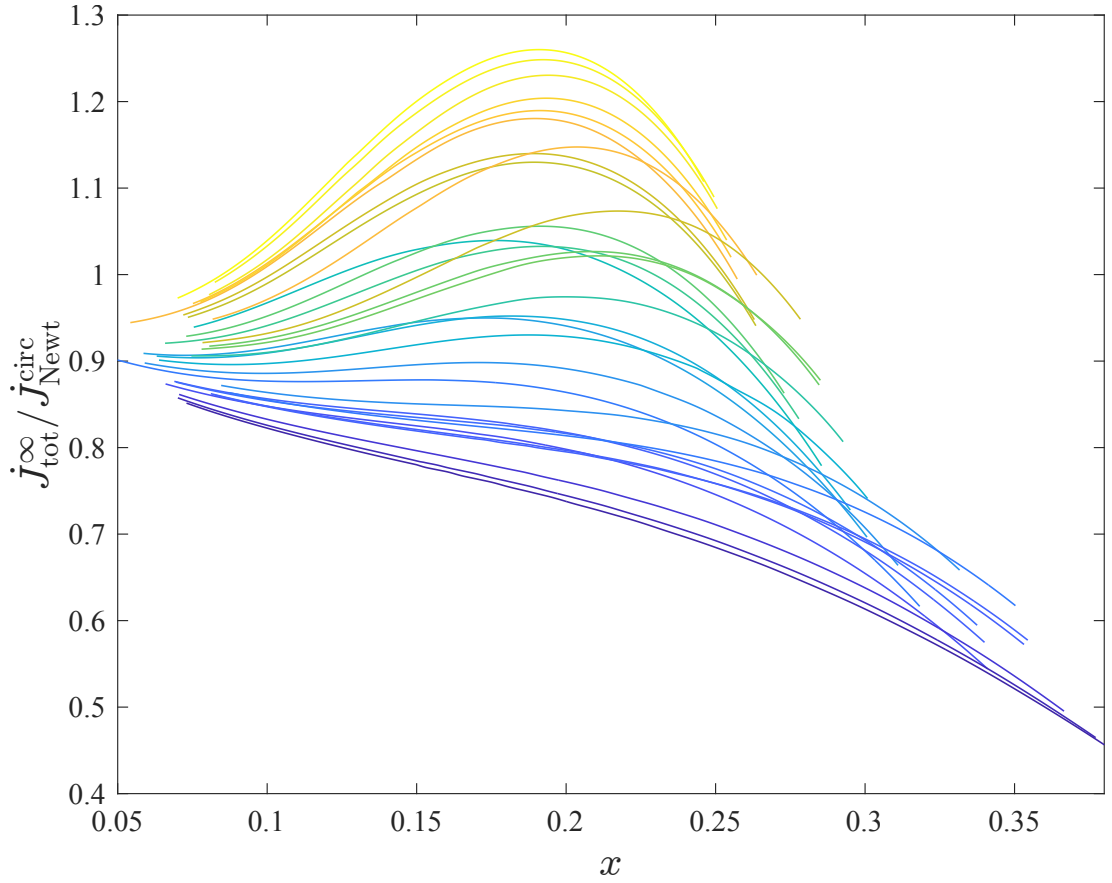

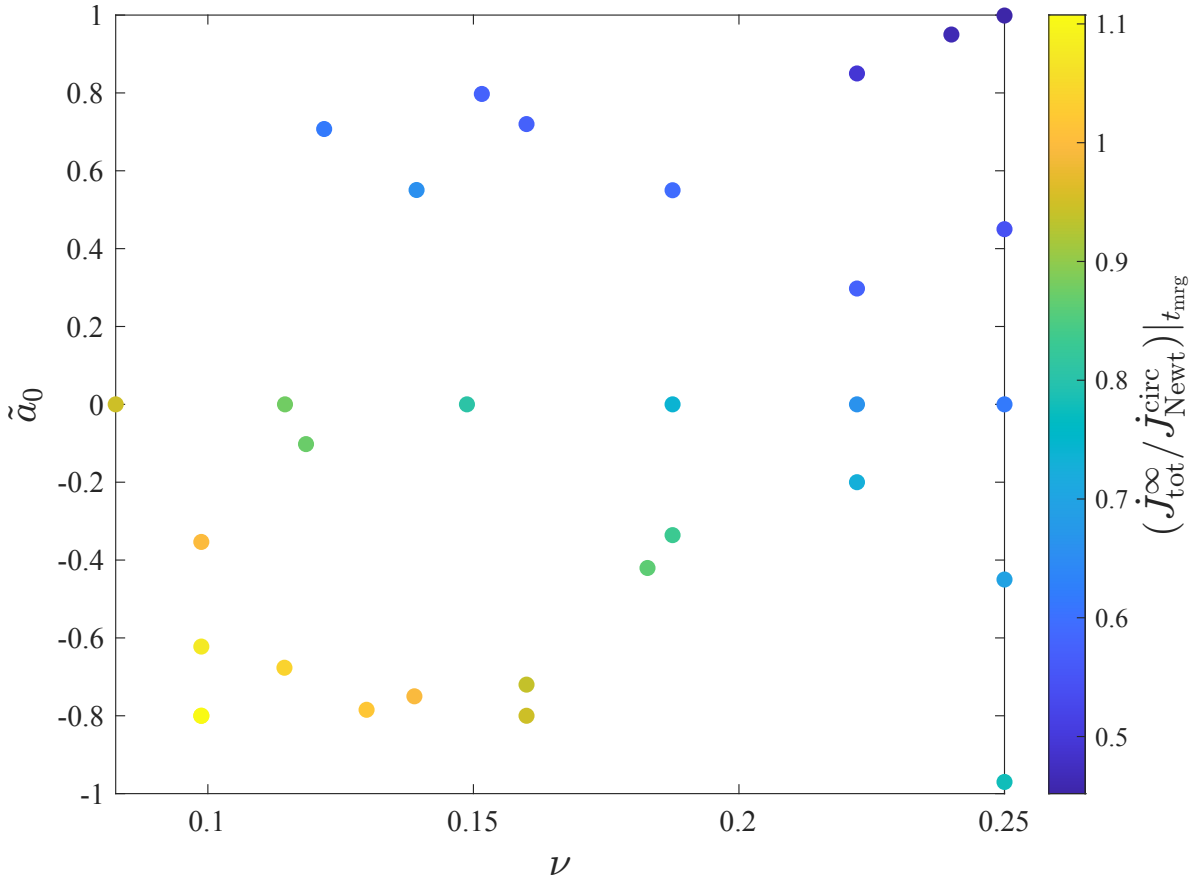

Output of the NR fluxes computation:

- comparable mass ratio / positive spins -> more adiabatic motion
- higher mass ratio / negative spins -> less adiabatic motion

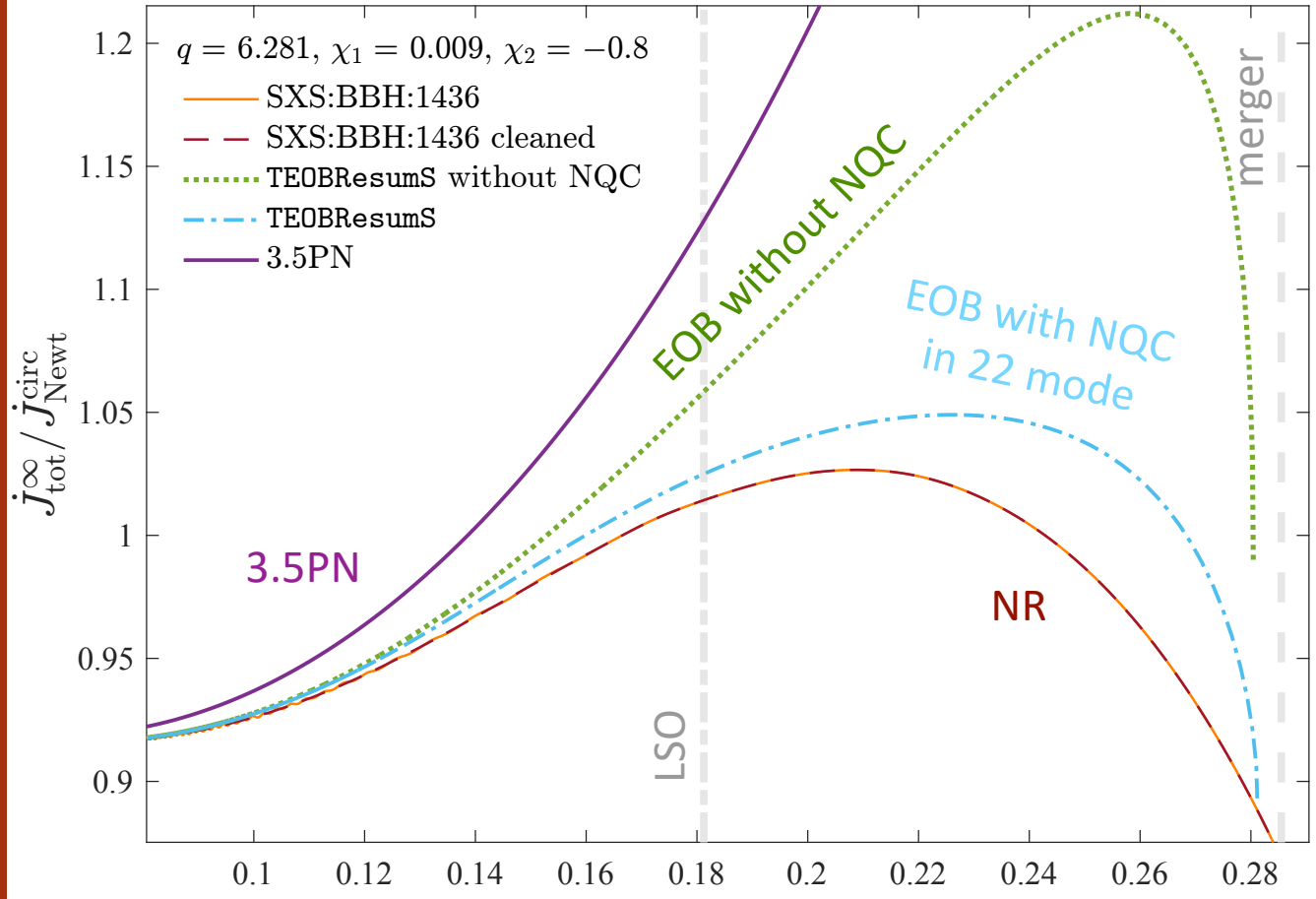

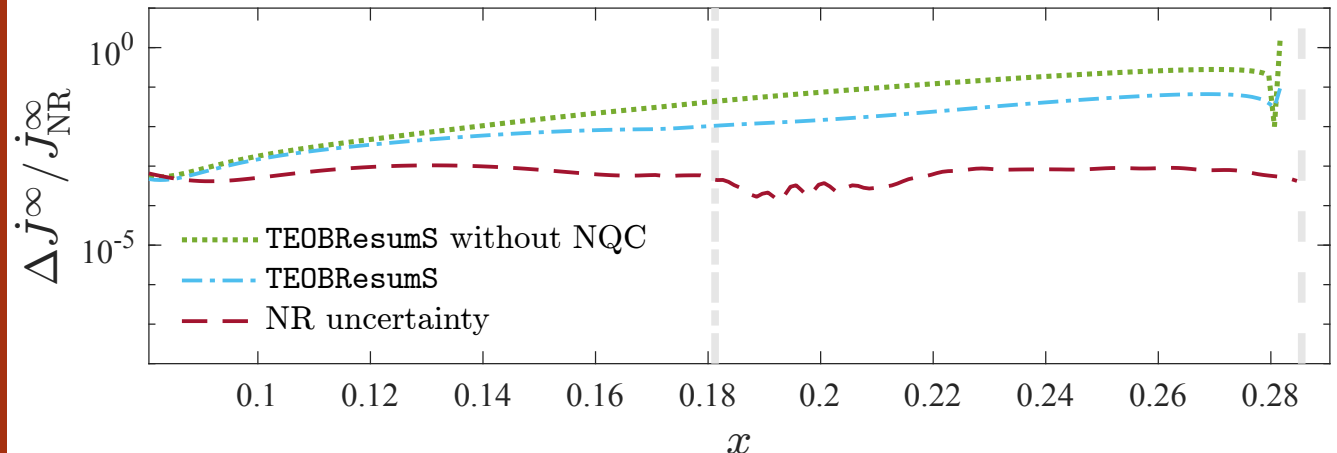

Comparing **total** fluxes

⬇

NQC corrections allow for a better agreement with **N**umerical **R**elativity

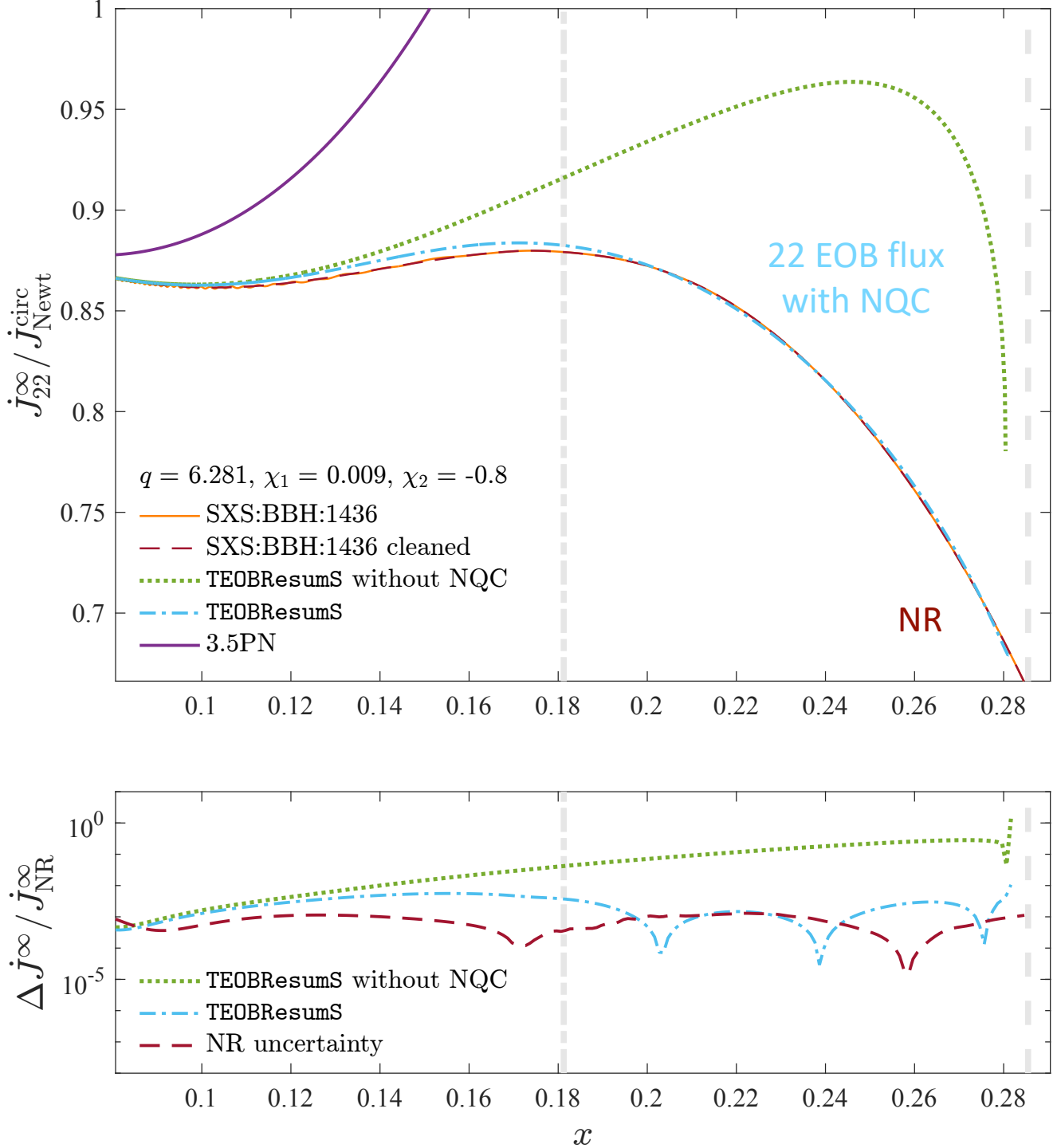

Comparing $\ell = m = 2$ fluxes

Robustness of the NQC correction factor for this mode

To increase the agreement of the **total** flux with Numerical Relativity we add NQC corrections in the $\ell = m = 3, 4, 5$ modes

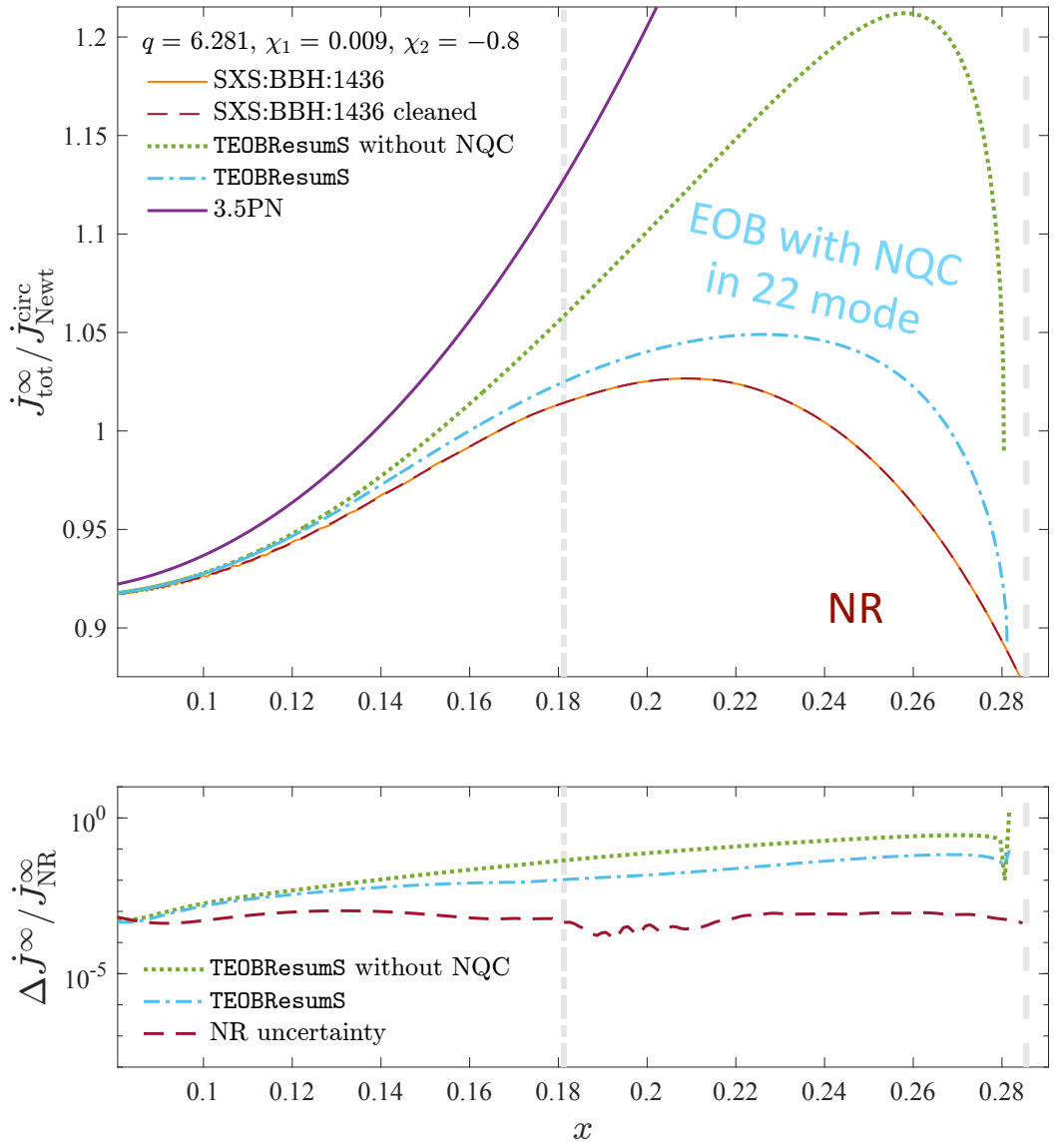

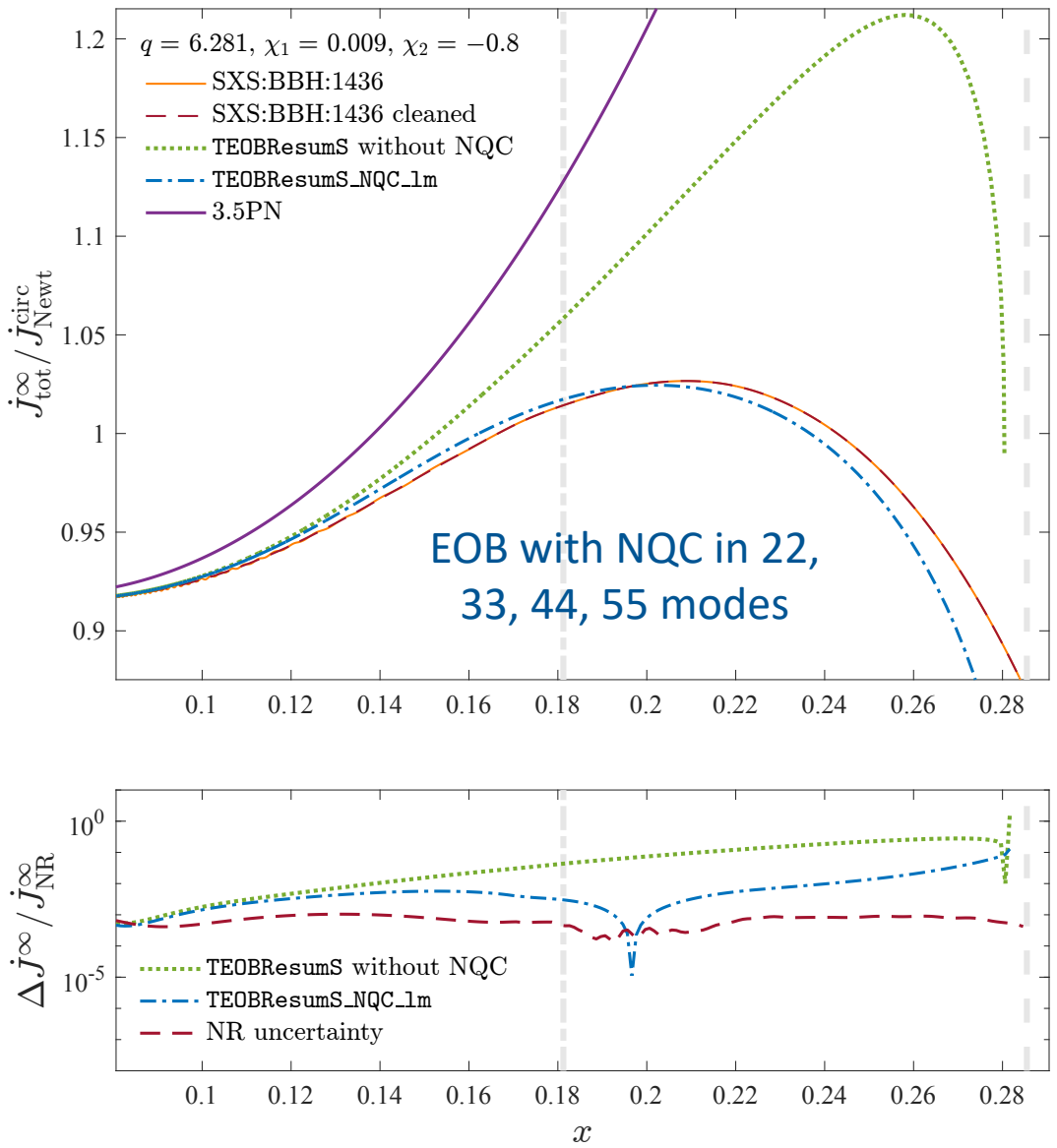

Having modified radiation reaction we had to re-calibrate the **spin-orbit** sector of the model…

New calibration of the effective spin-orbit parameter c_3

#	ID	(q, χ_1, χ_2)	$\tilde{a}_0$	$c_3^{\text{first guess}}$	c_3^{fit}
1	BBH:1137	$(1, -0.97, -0.97)$	-0.97	89.7	89.33
2	BBH:0156	$(1, -0.9498, -0.9498)$	-0.95	88.5	88.33
3	BBH:0159	$(1, -0.90, -0.90)$	-0.90	84.5	85.86
4	BBH:2086	$(1, -0.80, -0.80)$	-0.80	82	80.93
5	BBH:2089	$(1, -0.60, -0.60)$	-0.60	71	71.19
6	BBH:0150	$(1, +0.20, +0.20)$	$+0.20$	35.5	35.73
7	BBH:2102	$(1, +0.60, +0.60)$	$+0.60$	22.2	21.67
8	BBH:2104	$(1, +0.80, +0.80)$	$+0.80$	15.9	16.31
9	BBH:0153	$(1, +0.85, +0.85)$	$+0.85$	15.05	15.29
10	BBH:0160	$(1, +0.90, +0.90)$	$+0.90$	14.7	14.5
11	BBH:0157	$(1, +0.95, +0.95)$	$+0.95$	14.3	14.1
12	BBH:0177	$(1, +0.99, +0.99)$	$+0.99$	14.2	14.29
13	BBH:0004	$(1, -0.50, 0.0)$	-0.25	55.5	54.44
14	BBH:0005	$(1, +0.50, 0.0)$	$+0.25$	35	34.17
15	BBH:2105	$(1, +0.90, 0.0)$	$+0.45$	27.7	27.21
16	BBH:2106	$(1, +0.90, +0.50)$	$+0.70$	19.1	19.09
17	BBH:0016	$(1.5, -0.50, 0.0)$	-0.30	56.2	56.14
18	BBH:1146	$(1.5, +0.95, +0.95)$	$+0.95$	14.35	13.98
19	BBH:2129	$(2, +0.60, 0.0)$	$+0.40$	29.5	29.31
20	BBH:2130	$(2, +0.60, +0.60)$	$+0.60$	23	22.41
21	BBH:2131	$(2, +0.85, +0.85)$	$+0.85$	16.2	15.73
22	BBH:2139	$(3, -0.50, -0.50)$	-0.50	65.3	62.45
23	BBH:0036	$(3, -0.50, 0.0)$	-0.38	58.3	57.62
24	BBH:0174	$(3, +0.50, 0.0)$	$+0.37$	28.5	30.87
25	BBH:2158	$(3, +0.50, +0.50)$	$+0.50$	27.1	26.64
26	BBH:2163	$(3, +0.60, +0.60)$	$+0.60$	24.3	23.56
27	BBH:0293	$(3, +0.85, +0.85)$	$+0.85$	17.1	17.05
28	BBH:1447	$(3.16, +0.7398, +0.80)$	$+0.75$	19.2	19.46
29	BBH:2014	$(4, +0.80, +0.40)$	$+0.72$	21.5	21.52
30	BBH:1434	$(4.37, +0.7977, +0.7959)$	$+0.80$	19.8	20.05
31	BBH:0111	$(5, -0.50, 0.0)$	-0.42	54	57.18
32	BBH:0110	$(5, +0.50, 0.0)$	$+0.42$	32	30.98
33	BBH:1432	$(5.84, +0.6577, +0.793)$	$+0.68$	25	24.42
34	BBH:1375	$(8, -0.90, 0.0)$	-0.80	64.5	65.12
35	BBH:0114	$(8, -0.50, 0.0)$	-0.44	57	56.07
36	BBH:0065	$(8, +0.50, 0.0)$	$+0.44$	29.5	31.78
37	BBH:1426	$(8, +0.4838, +0.7484)$	$+0.51$	30.3	29.98

- Chose set of 37 simulations uniformly covering the parameter space
- First-guess values obtained aligning EOB waveforms to numerical ones in the time domain and minimizing the phase difference
- Changed functional form

$$c_3(\tilde{a}_1, \tilde{a}_2, \nu) = p_0 \frac{1 + n_1\tilde{a}_0 + n_2\tilde{a}_0^2 + n_3\tilde{a}_0^3 + n_4\tilde{a}_0^4}{1 + d_1\tilde{a}_0} + p_1\tilde{a}_0\nu\sqrt{1-4\nu} + p_2\left(\tilde{a}_1 - \tilde{a}_2\right)\nu^2$$

$$c_3(\tilde{a}_1, \tilde{a}_2, \nu) = p_0 \frac{1 + n_1\tilde{a}_0 + n_2\tilde{a}_0^2 + n_3\tilde{a}_0^3 + n_4\tilde{a}_0^4}{1 + d_1\tilde{a}_0} + p_1\tilde{a}_0\sqrt{1-4\nu} + p_2\tilde{a}_0^2\sqrt{1-4\nu} + p_3\tilde{a}_0\nu\sqrt{1-4\nu} + p_4\left(\tilde{a}_1 - \tilde{a}_2\right)\nu^2$$

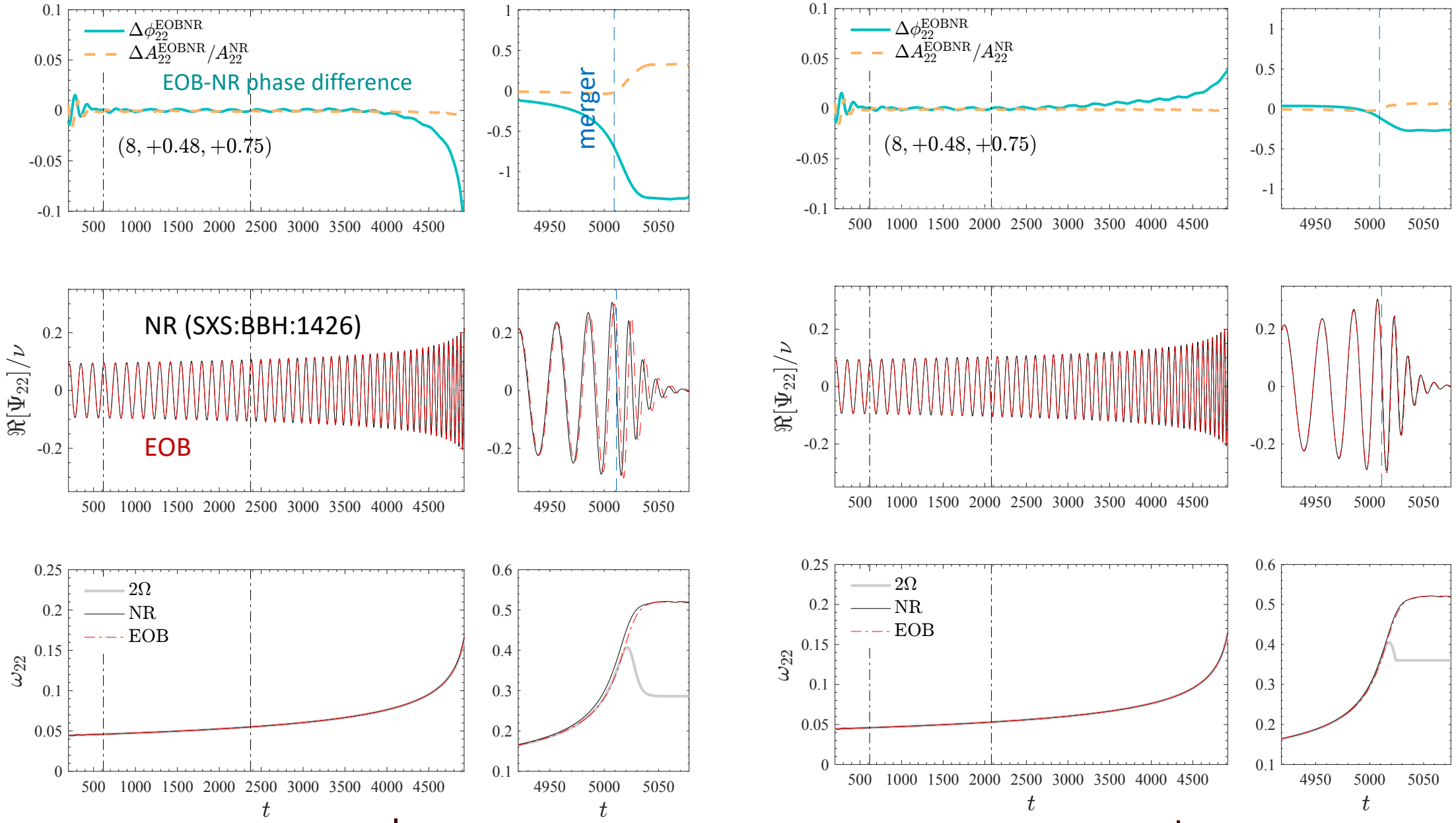

Old fit: $\Delta\phi_{22}^{\rm EOB-NR}\Big|_{\rm merger} = -0.70$

New fit: $\Delta\phi_{22}^{\rm EOB-NR}\Big|_{\rm merger} = -0.11$

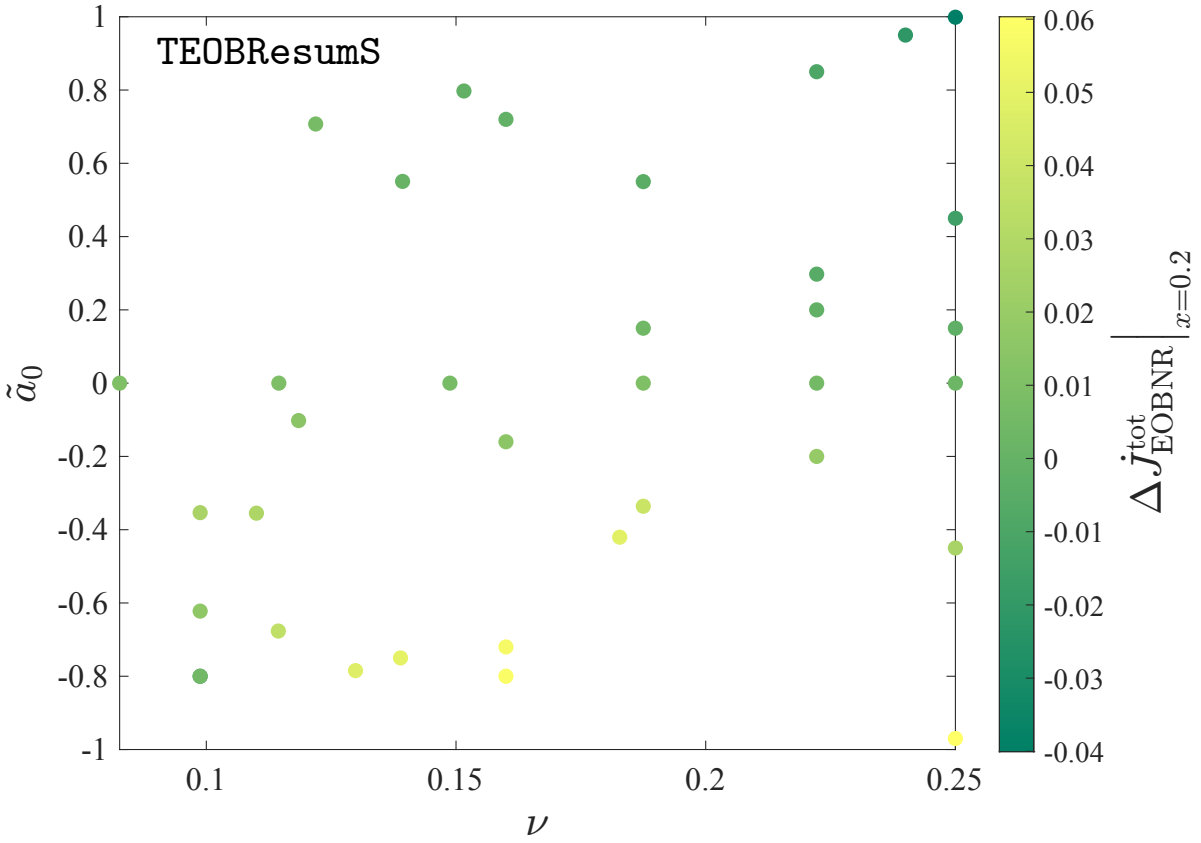

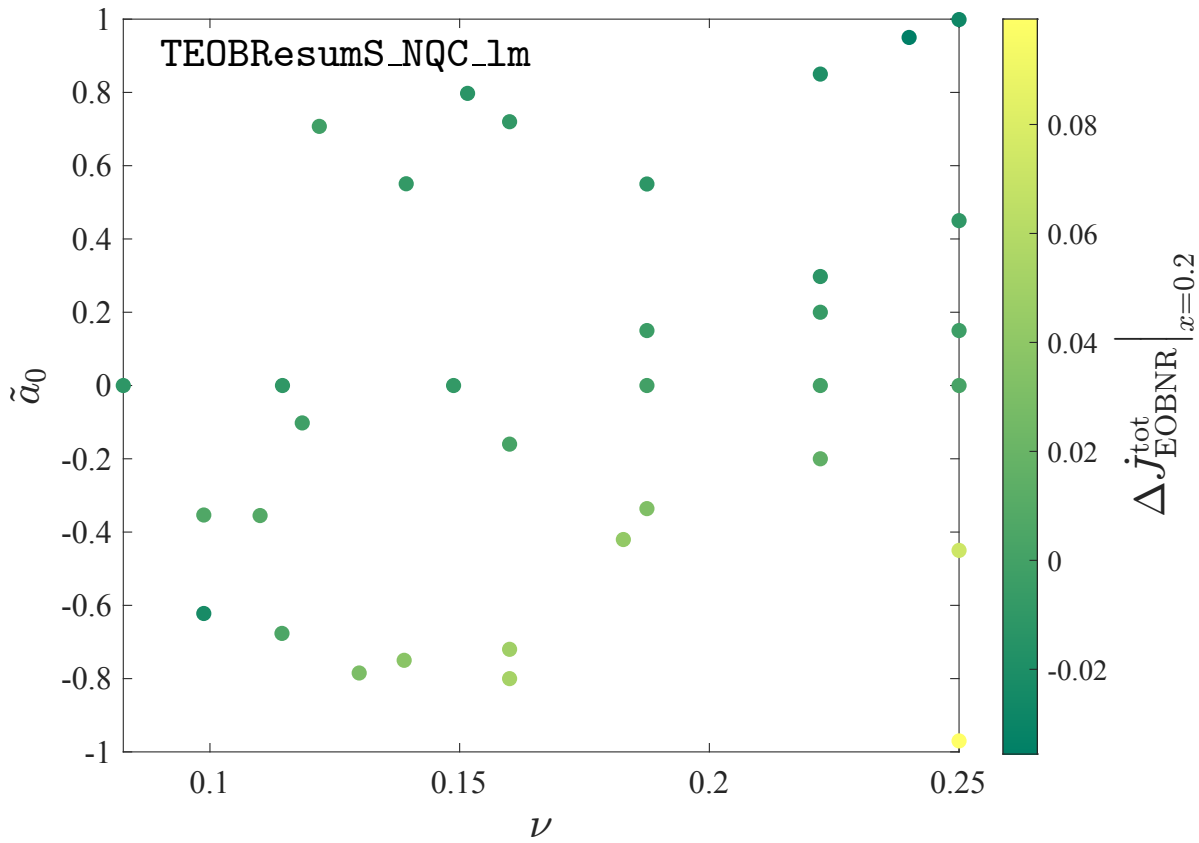

Relative (EOB - NR)/NR flux difference at $x = 0.2$

- lowered in the new model
- high negative spins remain the most problematic ones

Unfaithfulness: probing the reliability of the 22 mode

$$\bar{F}(M) \equiv 1 - F = 1 - \max_{t_0,\phi_0} \frac{\langle h_{22}^{\rm EOB}, h_{22}^{\rm NR}\rangle}{\|h_{22}^{\rm EOB}\|\|h_{22}^{\rm NR}\|} \qquad \|h\| \equiv \sqrt{\langle h,h\rangle} \qquad \langle h_1,h_2\rangle \equiv 4\Re\int_{f_{\rm min}^{\rm NR(M)}}^{\infty} \frac{\tilde{h}_1(f)\tilde{h}_2^*(f)}{S_n(f)}df$$

Zero-detuned high-power noise spectral density of Advanced LIGO

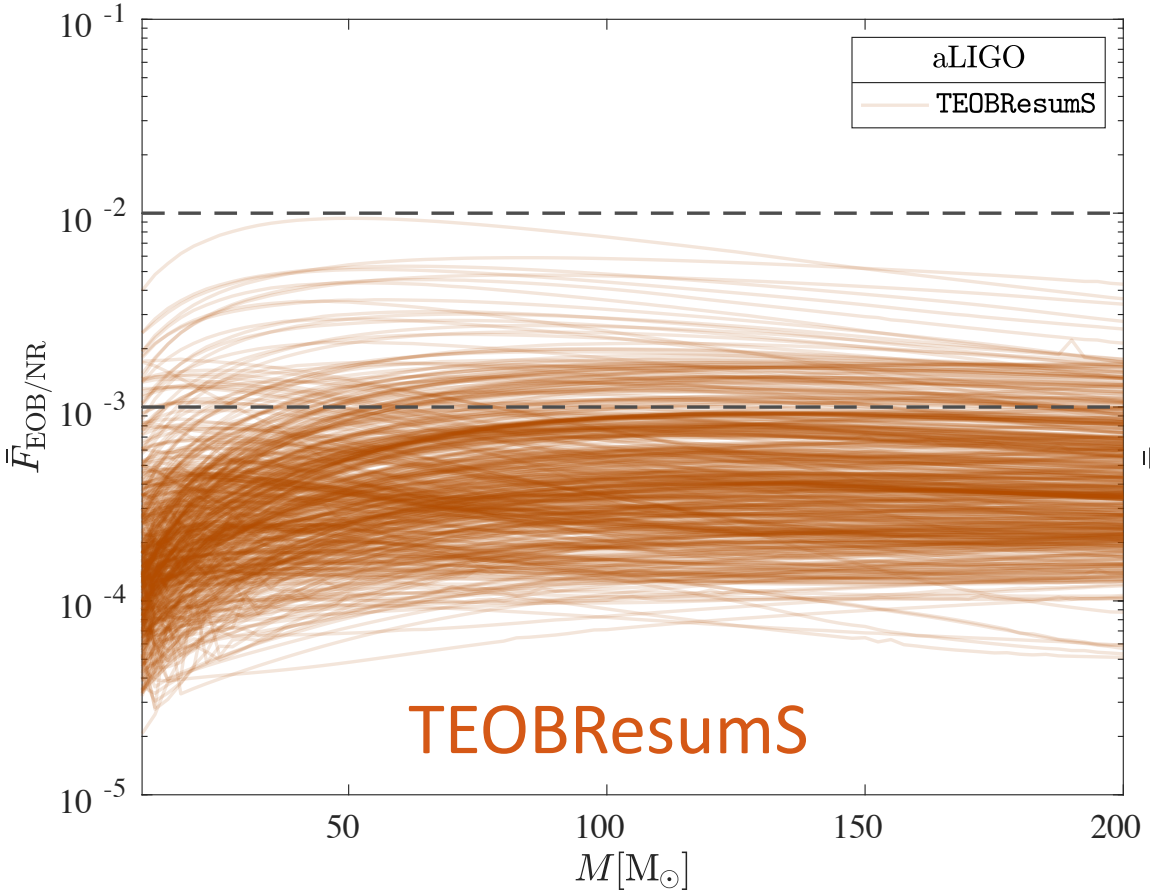

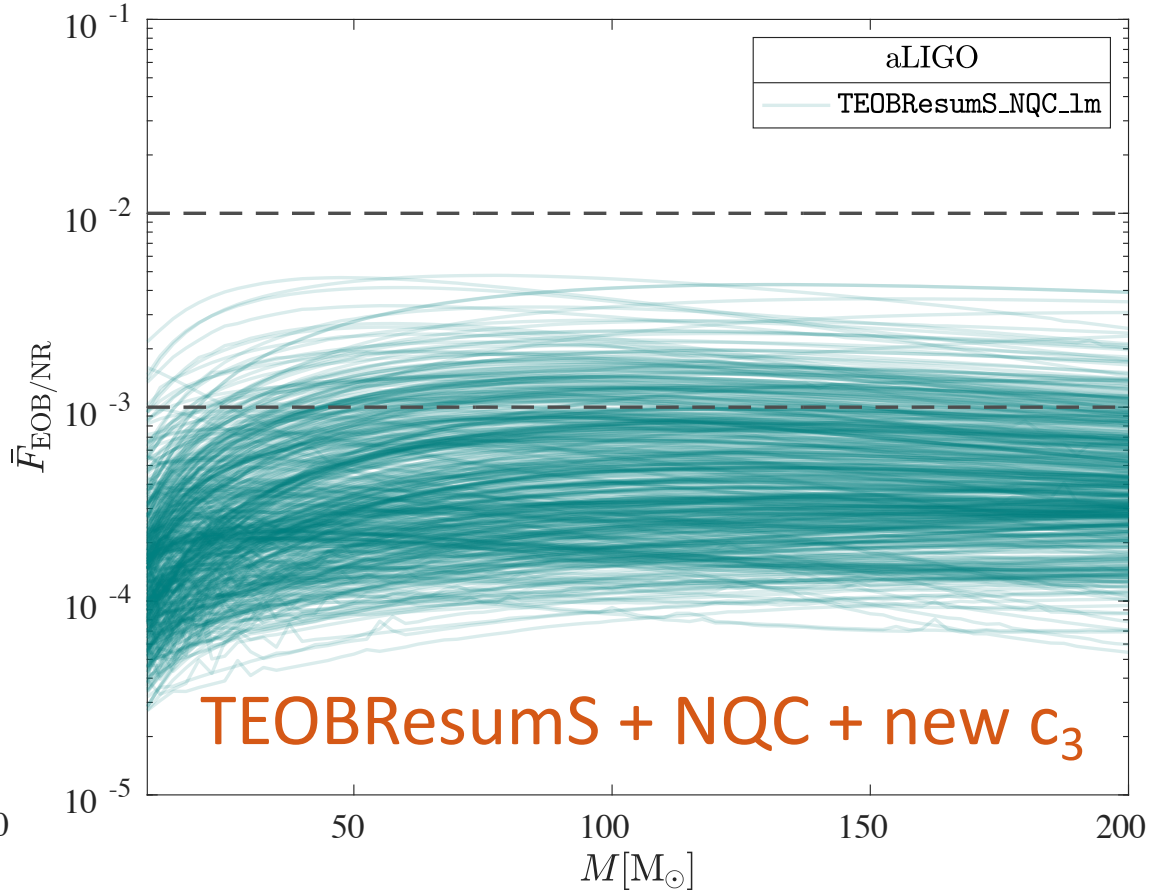

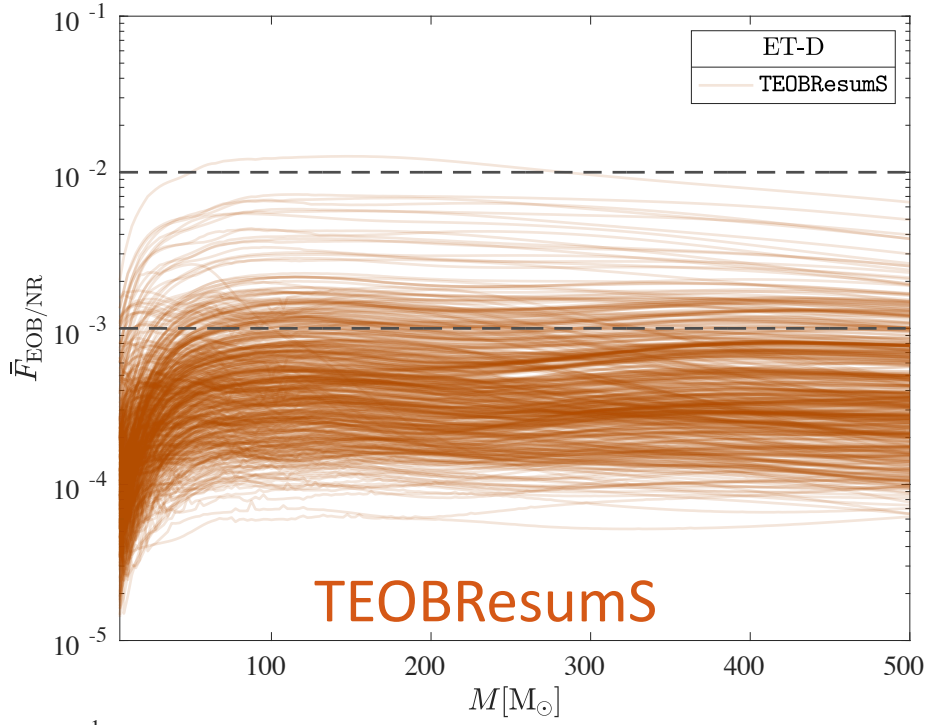

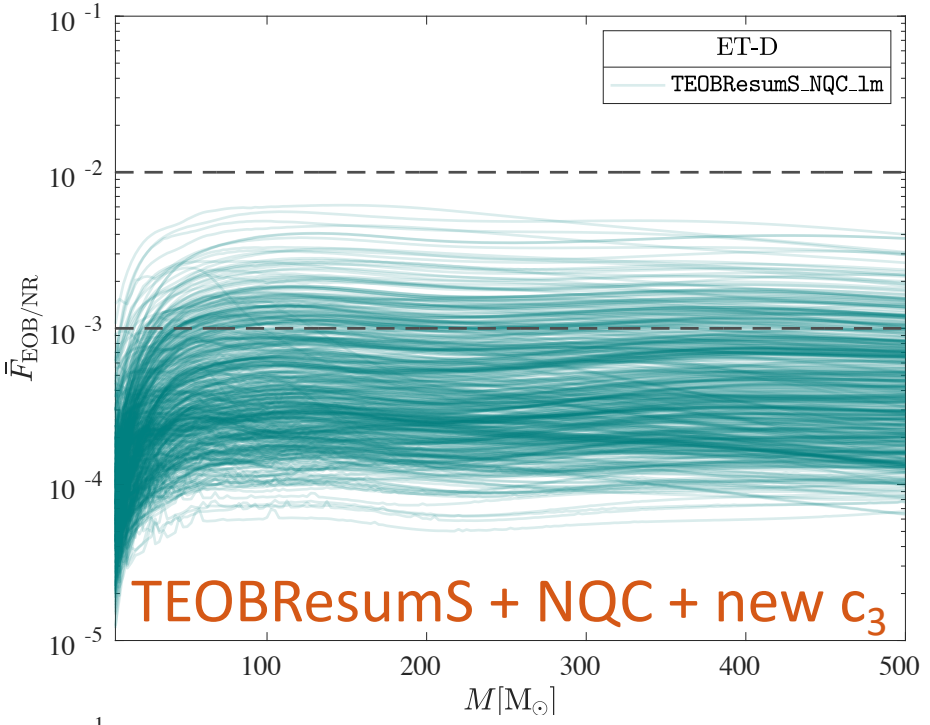

Einstein Telescope

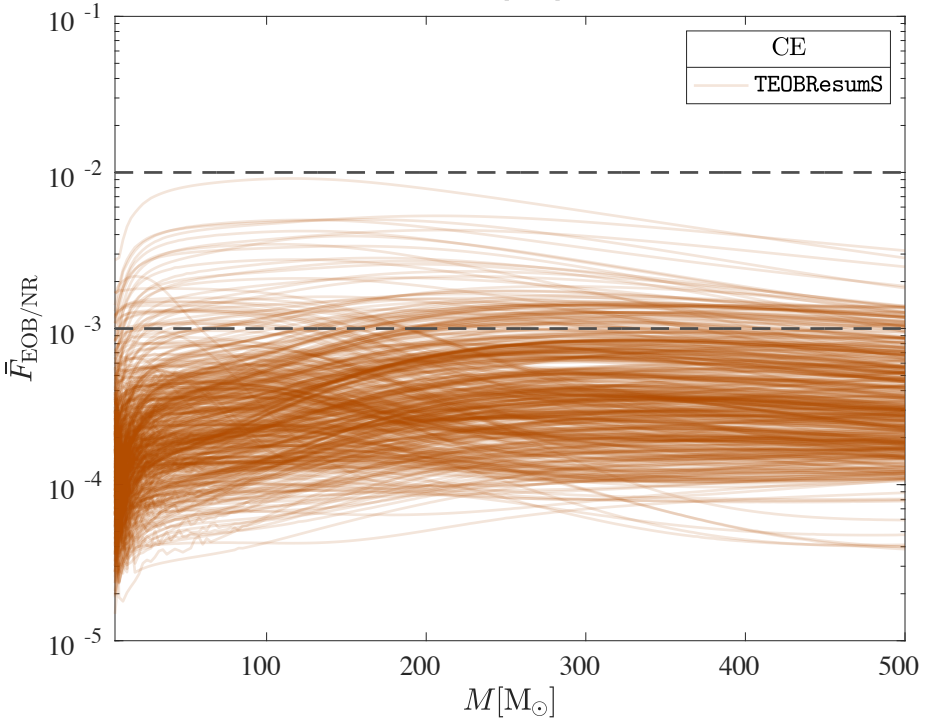

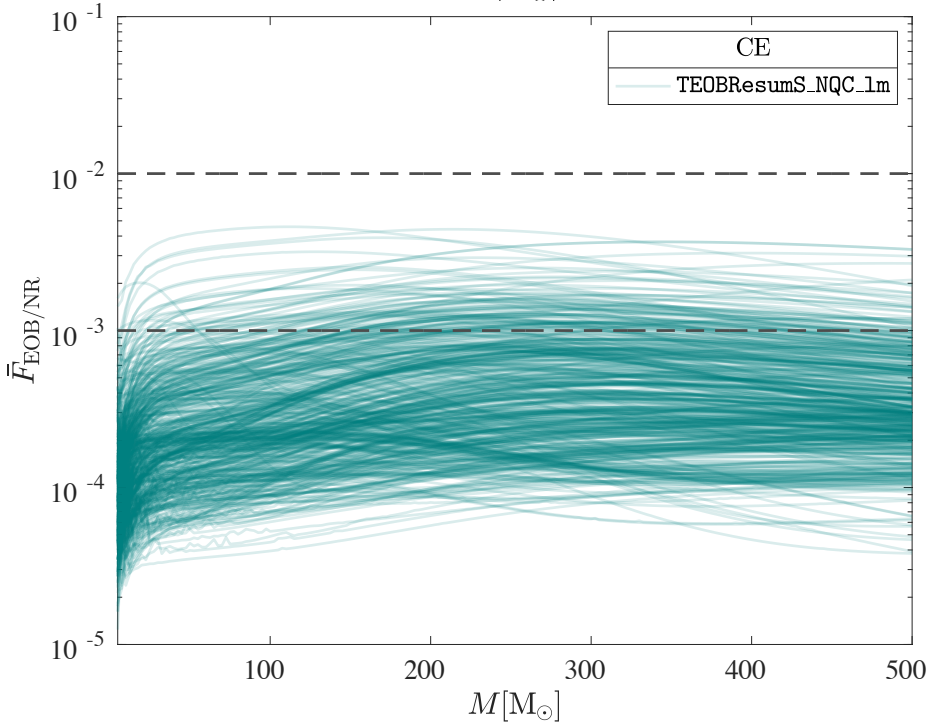

Cosmic Explorer

Almost reaching 10^{-5} for low masses, where the detector is mostly sensitive to the inspiral

From M. Pürrer and C.J. Haster. - **Gravitational waveform accuracy requirements for future ground-based detectors**. Phys. Rev. Res., 2(2):023151, 2020.

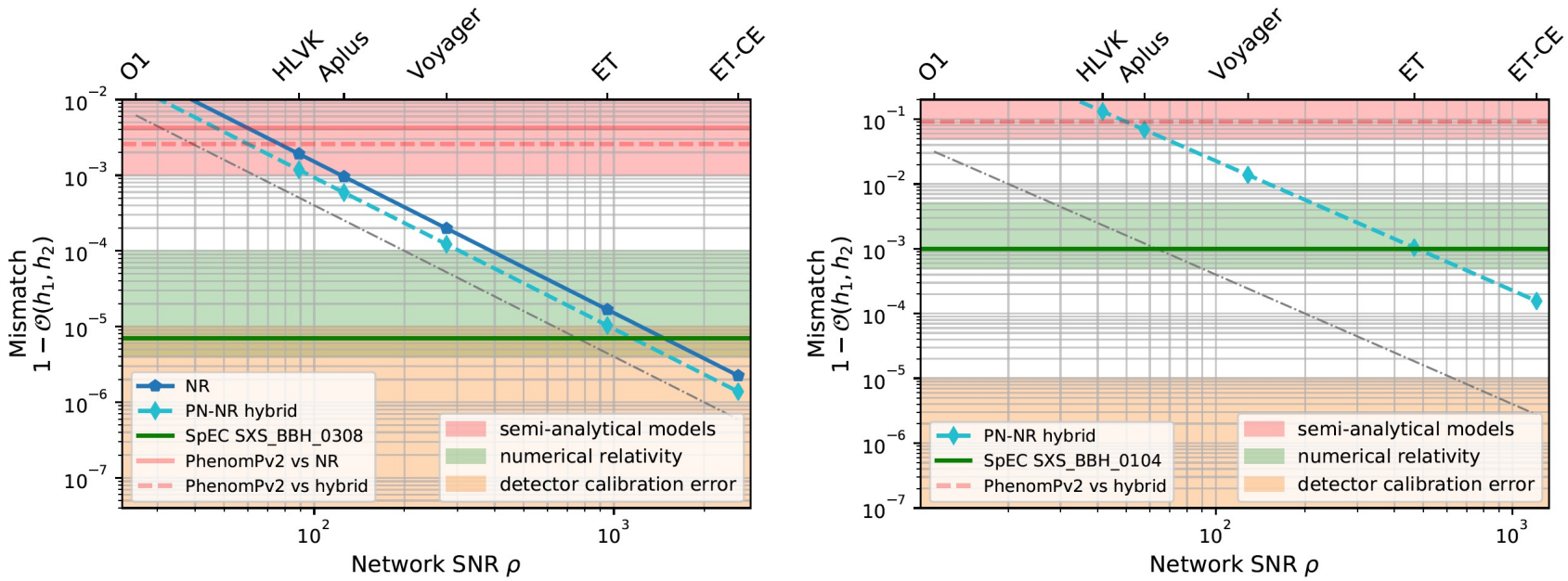

The semi-analytical models here considered (IMRPhenomPv2 and SEOBNRv4_ROM) are required to increase their accuracy of three orders of magnitude

The results of TEOBResumS suggest a more encouraging picture in view of next generation detectors

Conclusions

- TEOBResumS:
  - dynamical self-consistency
  - improved radiation reaction by agreement with numerical fluxes
  - re-informed the spin-orbit sector
  - good starting point for 3G detectors (and potentially for LISA)

- Space for improvement:
  - tuning to NR: different fits
  - incorporating more analytical information
    (e.g. higher PN orders, spinning particle terms in the Hamiltonian)
  - model for EMRIs: tuning to GSF